A REQUIREMENT FOR THE LYSINE METHYL TRANSFERASE SMYD1 IN MYOBLAST DIFFERENTIATION

A Dissertation Presented to

the Faculty of the Department of Biology and Biochemistry

University of Houston

In Partial Fulfillment

of the Requirements for the Degree

Doctor of Philosophy

By

Harika Nagandla

December 2015

A REQUIREMENT FOR THE LYSINE METHYL TRANSFERASE SMYD1 IN MYOBLAST DIFFERENTIATION

Harika Nagandla

APPROVED:

Dr. Robert J Schwartz, Chairman

Dr. M David Stewart, Co-chair

Dr. Dan Wells

Dr. Sang-Hyuk Chung

Dr. Bradley McConnell

Dean, College of Natural Sciences and Mathematics

ACKNOWLEDGEMENTS

I will always be grateful to Dr. Robert J. Schwartz for his guidance during my PhD program and also for providing funding as well as an opportunity to conduct research. I would like to express deep gratitude to Dr. M. David Stewart as this dissertation would have been impossible without his mentorship. His patience, attention-to-detail and meticulous approach have played a major role in shaping the researcher in me. I would like to thank the professors on my committee - Dr. Sanghyuk Chung, Dr. Bradley McConnell, and Dr. Dan Wells for their insightful feedback on my work. Special thanks to our technicians Wei Yu, Harry Wu, and Suhujey Lopez for their help with genotyping and embryo collection. I am indebted to my parents N. V. R Murthy and Adilaxmi Nagandla, my sister Sonika Nagandla, and my dear friends - Ashwini Shanbhogue, Sneha Lal, Udyana Gyada, and Tanvi Patil as their kind words of support and encouragement kept me going during tough times. I cannot thank my friends Nick Valenzuela and Jong Kim enough, for making the atmosphere in the lab jovial and also for broadening my perspective on numerous things in and out of the lab. I would also like to thank all the members of our extended Schwartz lab family, daily interactions with whom helped me grow as a researcher and made the past five years a delightful experience.

A REQUIREMENT FOR THE LYSINE METHYL TRANSFERASE SMYD1 IN MYOBLAST DIFFERENTIATION

An Abstract of a Dissertation

Presented to

the Faculty of the Department of Biology and Biochemistry

University of Houston

In Partial Fulfillment

of the Requirements for the Degree

Doctor of Philosophy

By

Harika Nagandla

December 2015

ABSTRACT

The SMYD (SET and MYND domain) family of lysine methyltransferases harbors a unique structure in which the methyltransferase (SET) domain is intervened by a zinc finger protein-protein interaction (MYND) domain. SMYD family proteins methylate both histone and non-histone substrates and participate in diverse biological processes including transcriptional regulation, DNA repair, proliferation, and apoptosis. *Smyd1* is unique among the five family members in that it is specifically expressed in striated muscles. Complete deletion of *Smyd1* in mice caused embryonic lethality at E10.5 due to defects in heart development prior to proper onset of skeletal myogenesis program. *Smyd1* is expressed in the skeletal muscle lineage throughout myogenesis and in mature myofibers, shuttling from nucleus to cytosol during myoblast differentiation. Because of this expression pattern, we hypothesized that Smyd1 plays multiple roles at different stages of myogenesis. The goal of our study was to decipher Smyd1's role in mammalian skeletal muscle development. This was achieved by using Myf5-cre to knock *Smyd1* out of earliest skeletal muscle precursor cells, thereby providing clues to its nuclear function. We found that *Smyd1* is dispensable for initiation of skeletal myogenesis and *Smyd1* conditional knock-out (CKO) embryos appear unaffected during the primary myogenic wave. However, by the second myogenic wave, both primary and secondary muscle fibers in *Smyd1* CKO

embryos had declined in number with no change in myoblast proliferation or apoptosis as compared to control embryos. A number of skeletal muscle-specific genes were found to be down-regulated at the mRNA level in *Smyd1* CKOs by the secondary wave of myogenesis. Also, *Smyd1* CKO embryos exhibited significantly higher percentage of $Myog^{+}$ cells in the EDL during the second wave of myogenesis, indicating a block in downstream differentiation. Mutant embryos showed perinatal lethality and subcutaneous edema. Down-regulation of Smyd1 in C2C12 skeletal myoblast cell-line led to poorly differentiated, thinner myotubes, thereby recapitulating our observations *in-vivo*. Smyd1 appears important for proper down-stream differentiation of skeletal myoblasts.

Table of Contents

List of Figures

List of tables

Chapter I

Literature Review

Somitogenesis

Skeletal muscle is the most abundant tissue in the vertebrate body. Most skeletal muscles of the body, except for the cranio-facial muscles arise from somites during embryogenesis (Biressi et al., 2007a). Somites are transient, condensed blocks of paraxial mesoderm, flanking the neural tube and developing in rostro-caudal succession (Fig. 1). Each somites consists of three specialized compartments (Fig. 2). The dorsal portion of the somite becomes the dermomyotome, which is epithelial in nature and gives rise to skin (dermis) (Biressi et al., 2007a). The ventral portion of the somite undergoes epithelial-mesenchymal transition (EMT) and becomes the sclerotome, which consists of precursors for ribs and vertebrae (Wagner et al., 2000). The region in between the dermomyotome and sclerotome is the myotome (Fig. 2), containing precursor cells for all skeletal muscle of the body. The somite is further classified into epaxial (dorsal to the neural tube) and hypaxial (ventral to the neural tube) domains depending on the anatomical positioning. The epaxial domain of the somite gives rise to muscles of the trunk whereas limbs, diaphragm and ventral body wall develop from the hypaxial domain (Wagner et al., 2000).

Signaling pathways from adjacent tissues play an important role in somitogenesis. Wnts secreted from surface ectoderm and dorsal neural tube as well as Sonic hedgehog (Shh) released from neural tube floor plate (Fig. 2) and notochord are required for proper specification muscle progenitor cells in the somite (Bentzinger et al., 2012). On the other hand, Bone morphogenetic protein (BMP) and Notch signaling pathways serve to maintain sufficient pool of myogenic precursor cells while inhibiting downstream differentiation (Bentzinger et al., 2012).

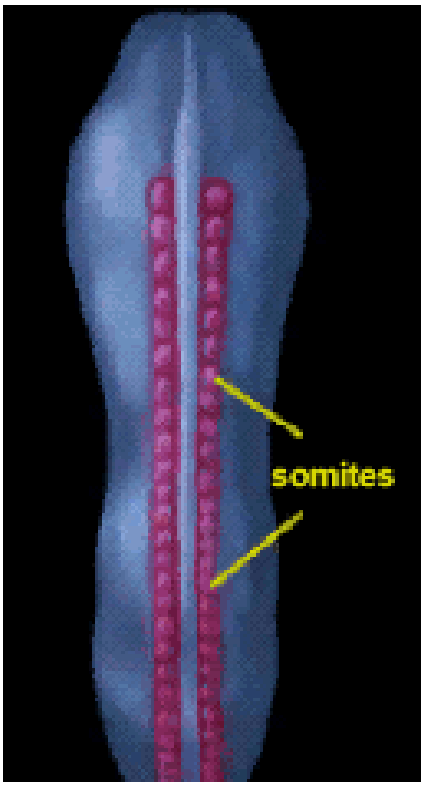

Fig. 1 Newly formed somites (red blocks) flanking the neural tube in a developing vertebrate embryo

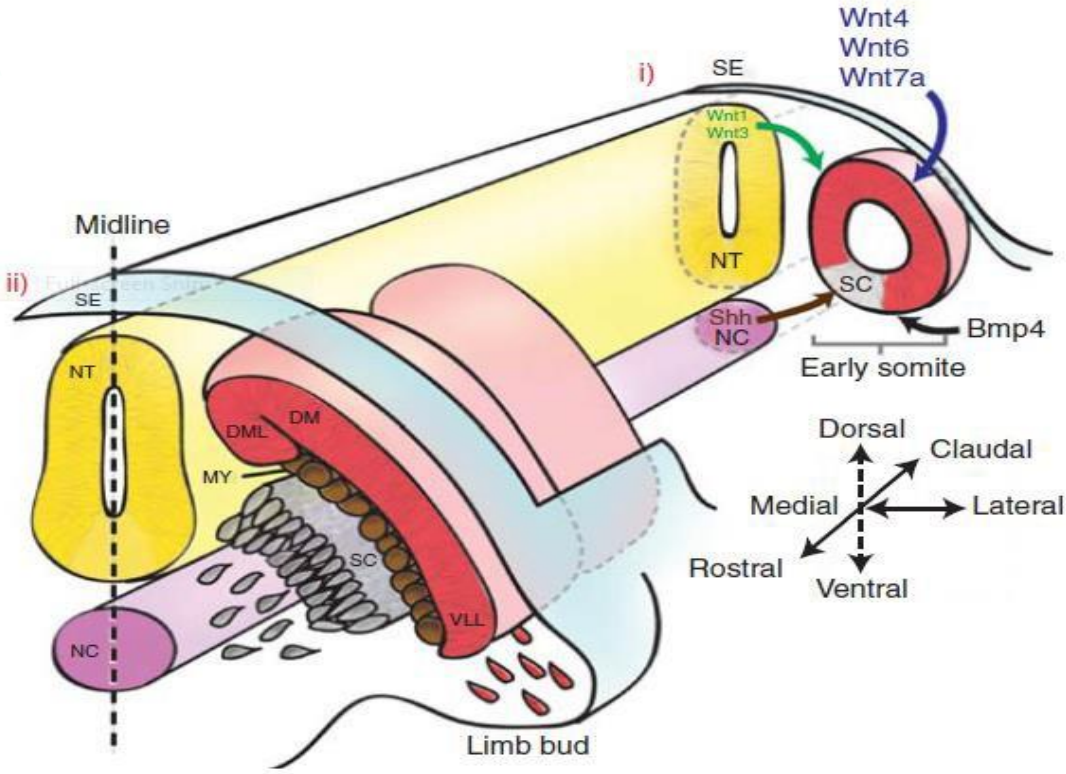

C. Florian Bentzinger et al. Cold Spring Harb Perspect Biol 2012;4:a008342

Fig. 2 Signals such as Wnts, Sonic hedge hog (Shh) from surface ectoderm (SE), notochord (NC) and dorsal neural tube (NT) are important for proper specification of the myogenic progenitors (i). Transverse section of a somite showing three compartments - dermo-myotome, myotome and sclerotome (ii)

Myogenic regulatory factors (MRFs) – Structure

MRFs consist of four members - Myf5, Myf6, MyoD and MyoG. The MRFs are a family of transcriptional factors crucial for the skeletal myogenesis program and were first identified for their ability to cause non-muscle cells such as fibroblasts to fuse into myotubes upon ectopic expression. All four MRFs are conserved in structure. They consist of three conserved domains - N-terminal transactivation domain rich is histidine and cysteine residues, basic helix-loop-helix (bHLH) domain in the center that facilitates hetero-dimerization with E proteins and C-terminal amphipathic α-helix domain also involved in transactivation (Comai et al., 2014). The bHLH domain recognizes the E-box element 'CANNTG' in the regulatory region of target genes to modulate their transcriptional activity. The bHLH domain is highly conserved in vertebrates from fish to humans, leading to the hypothesis that all four MRFs may have been derived from the same ancient gene and could be the result of two rounds of gene duplication (Comai et al., 2014).

Myogenic regulatory factors (MRFs) – Knock out studies in mice

Myf5 is the first MRF to be expressed in the myotome of mouse embryo at E8. It is also expressed in the ribs, adipogenic and neuronal cells. Expression of MyoG at E8.5, Myf6 at E9 and MyoD at E10.5 follows that of Myf5 during embryogenesis (Francetic et al., 2011). Contributions of MRFs to skeletal myogenesis have been deduced through several knock-out studies in mice. Remarkably, Myf5 null mice did not exhibit any defects in skeletal myogenesis program, except for delayed appearance of myotomal cells until MyoD expression started. However, Myf5 null mice are perinatal lethal due improper development of distal ribs and inability to breathe. Similarly MyoD null mice also showed normal skeletal muscle development with prolonged and higher expression of Myf5. Double knock-out of Myf5 and MyoD led to mice with absence of skeletal myoblasts and lack of skeletal muscle. Since Myf5 and Myf6 are closely located on chromosome 10, it was later found that Myf6 expression had also been disrupted in Myf5-MyoD double knock-out mice. Hence in effect these mice harbored triple knock-out of Myf5, Myf6 and MyoD, which came to be labeled as myogenic commitment factors due to the fact that there was a complete loss of skeletal myoblasts in their absence. Newer model of Myf5-MyoD double knock-out while retaining Myf6 expression showed that myogenesis proceeds normally. Myogenin (MyoG) null mice exhibit perinatal lethality with

fewer myofibers and although skeletal myoblasts are present, they fail to fuse into myotubes. Myf6-MyoD double knockout mice have the same phenotype as MyoG null mice. Three knock-outs have been carried out for Myf6 with phenotypes varying from normal skeletal muscle development and no lethality to some muscle defects with perinatal lethality. Increased expression of MyoG and defects in deep back muscles led to the conclusion that Myf6 is important for terminal differentiation of myoblasts (Francetic et al., 2011). This led to the inference that MyoG, MyoD and Myf6 function as differentiation factors for myoblasts.

Myoblast Differentiation

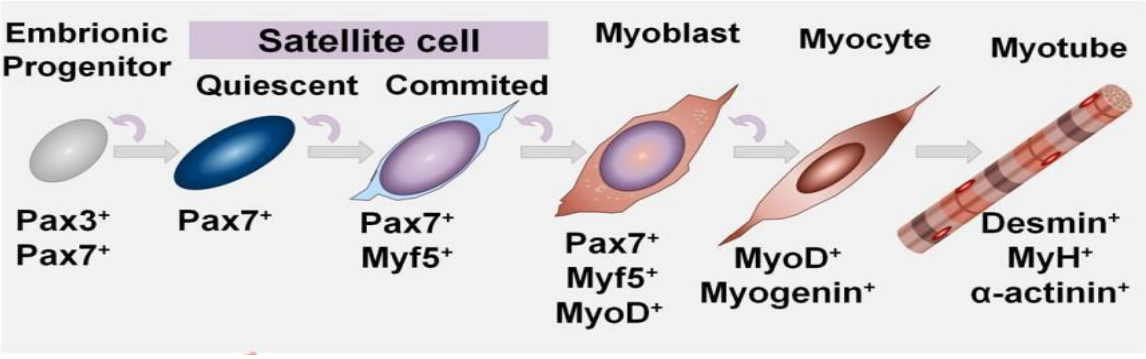

Skeletal Muscle Regeneration for Clinical Application, Regenerative Medicine and Tissue Engineering (2013)

Fig. 3 Differentiation pathway of a myoblast showing intermediate phases marked by expression of important transcription factors

The earliest muscle precursor cells in the myotome of a developing mouse embryo can be identified by the expression of Pax3 and Pax7. A myogenic progenitor cell expressing Pax3 and Pax7 can either differentiate to become a satellite cell or undergo further downstream differentiation to become a myoblast (Fig. 3). Satellite cells marked by the expression of Pax7 function as muscle tissue specific stem cells in the adult mice and participate in repair and regeneration of skeletal muscle. Myf5 and MyoD are earliest transcription factors to be expressed in proliferating myoblasts (Fig. 3). These myoblasts differentiate into myocytes after they exit the cell cycle. Myocytes are mono-nucleated, non-proliferating, terminally differentiated muscle cells governed by the expression of MyoG (Myogenin) and Myf6. Later these myocytes fuse to form multi-nucleated myotubes, marked by the expression of cyto-skeletal proteins such as Actin and Desmin (Fig. 3). Hence the journey of a cell from being an embryonic progenitor to being incorporated into a myotube consists of several intermediate phases each of which can be identified by the expression of one or two transcription factors, that push the cell downstream into the differentiation pathway and then their expression drops. For example, once a progenitor cell differentiates into a myoblast, Pax3 expression is no longer required. Similarly, Myf5 expression is shut-down when myoblasts withdraw from cell-cycle and differentiate into myocytes and MyoG (Myogenin) expression declines upon formation of myotubes by fusion of myocytes.

Chapter II

Introduction

INTRODUCTION

Congenital myopathies and muscular dystrophies arise from genetic mutations in genes responsible for diverse aspects of myogenesis and myofiber homeostasis. Thus, understanding the molecular genetics of muscle development is paramount to developing the basic science foundation required to develop cures for these diseases. Mammalian embryonic skeletal myogenesis consists of two distinct phases producing primary and secondary myofibers, respectively. In mice, the primary/embryonic wave takes place from embryonic day (E) 10.5 to E12.5 and the secondary/fetal wave occurs from E14.5 to E17.5 (Biressi et al., 2007b). Primary muscle fibers first appear on E11.5, when a small fraction of embryonic myoblasts fuse. Secondary fibers are formed through fusion of fetal myoblasts with each other or with primary fibers. From E15.5 onwards, smaller secondary fibers can be found adjacent to bigger primary fibers, budding off of them. Fetal myogenesis is also characterized by inception of innervation (Rossi and Messina, 2014). The myogenic cells that give rise to these two waves have been well documented to have distinct characteristics in terms of the genes they express, the features of the myotubes they produce *in vitro* and their response to inhibitors of myogenesis and growth factors (Biressi et al., 2007b). In general, primary fibers are similar to adult slow-twitch muscle fibers while secondary

fibers exhibit characteristics of adult fast-twitch muscle fibers (Biressi et al., 2007a).

The SMYD (SET and MYND domain) family of lysine methyltransferases is defined by a unique structure in which the methyltransferase (SET) domain is intervened by a protein-protein interaction MYND domain (Spellmon et al., 2015). SMYD proteins are implicated in a vast number of biological processes including transcriptional activation/repression (Huang et al., 2006; Xu et al., 2015), DNA repair (Piao et al., 2014), cell cycle (Cho et al., 2012; Saddic et al., 2010), tumorigenesis (Luo et al., 2014; Mazur et al., 2014) and apoptosis (Sajjad et al., 2014). *Smyd1* is unique from the four other family members in that it's expression (*a* and *b* isoforms) is restricted to striated muscles; a third *c* isoform is expressed in $CD8^+$ T cells (Gottlieb et al., 2002; Hwang and Gottlieb, 1997). Smyd1 harbors both transcriptional activation and repression activities and methylates both histone and non-histone substrates (Rasmussen et al., 2015; Tan et al., 2006). Smyd1 methylates histone H3 at lysine 4, a modification associated with active transcription (Tan et al., 2006). Smyd1 represses transcription when tethered to DNA by recruitment of HDAC1, -2 or -3 to its MYND domain (Sims et al., 2002). The MYND domain is also the site of interaction with the muscle-specific transcription factor skNAC (Sims et al., 2002), the only transcription factor known to associate with Smyd1. Smyd1

methylates the cardiac endoplasmic reticulum stress sensor TRB3, which in turn, serves as a co-repressor for Smyd1 (Rasmussen et al., 2015). Expression of *Smyd1* in muscle is regulated by a number of factors such as Mef2C, SRF, Myogenin and HDGF (Li et al., 2009; Phan et al., 2005; Yang and Everett, 2009). Conventional knockout of *Smyd1* in mice results in embryonic lethality by E10.5 due to failure in right ventricular development (Gottlieb et al., 2002).

Due to embryonic lethality prior to myogenesis in mice (Gottlieb et al., 2002), most knowledge of Smyd1's function in skeletal muscle comes from studies in zebrafish (Du et al., 2006; Gao et al., 2014; Li et al., 2011; Li et al., 2013; Tan et al., 2006) where it is critical for sarcomerogenesis in fast-twitch muscles (Just et al., 2011). Smyd1 co-localizes with nascent myosin during sarcomerogenesis and then to the M-line of mature sarcomeres. Antisense morpholino-based knock-down of both *Smyd1* isoforms in zebrafish embryos led to severe impairment of myofibrillogenesis in both skeletal and cardiac muscle. Myosin chaperones *Hsp90α1* and *UNC45b* were up regulated (Just et al., 2011; Li et al., 2013), leading to the idea that Smyd1 stabilizes thick filament assembly. Smyd1's physical interaction with myosin is crucial for proper myofibrillar arrangement in zebrafish skeletal muscle (Just et al., 2011). These data indicate that Smyd1 is an important facilitator of myofibrillogenesis.

Based on gene expression and protein localization, we hypothesized that *Smyd1* also plays a role in early myogenesis. In *Xenopus laevis*, chicken and zebrafish embryos, *Smyd1* is expressed in the somites at the onset of myogenesis (Du et al., 2006; Gottlieb et al., 2002; Just et al., 2011; Kawamura et al., 2008). Expression persists throughout myogenesis and in mature myofibers. The subcellular localization of Smyd1 during myogenesis has been studied *in vitro* using mouse C2C12 myoblasts (Sims et al., 2002). In C2C12 cells, *Smyd1* expression increases tremendously during the transition from myoblast to myotubes (Berkholz et al., 2014; Li et al., 2009; Sims et al., 2002). Smyd1 localizes to the nucleus and cytoplasm of myoblasts; however, after fusion, Smyd1 mostly resides in the cytoplasm of myotubes (Berkholz et al., 2014; Sims et al., 2002). This nuclear to cytoplasmic translocation of Smyd1 during myoblast differentiation is regulated by sumoylation—as inhibition of sumoylation resulted in nuclear accumulation of Smyd1 and reduced terminal differentiation (Berkholz et al., 2014). These data suggest a role for Smyd1 in the formation of myotubes during embryogenesis.

The purpose of this study was to elucidate Smyd1's role during skeletal myogenesis in mice. To this end, we conditionally eliminated *Smyd1* from early muscle precursor cells using *Myf5*^{cre}. Deletion of *Smyd1* in early myoblasts did not affect myoblast abundance or proliferation, but did result in down-regulated

transcription of skeletal muscle-specific genes and fewer muscle fibers. Muscular defects were temporally restricted to the second myogenic wave, possibly due to a defect in terminal differentiation of myoblasts. Thus, in addition to the previously described functions for Smyd1 in expansion of second heart field progenitor cells, maturation of cardiomyocytes, antagonizing cardiomyocyte stress responses and skeletal muscle sarcomerogenesis, these results point to a novel role for Smyd1 in myoblast differentiation.

Chapter III

Results

RESULTS

Smyd1 expression and subcellular localization during myogenesis. A previous analysis of *Smyd1* spatial expression during embryogenesis showed *Smyd1* mRNA to be expressed very specifically in the heart and somites of chick embryos by Hamburger and Hamilton stage 20 (Gottlieb et al., 2002). Similar expression was reported for zebrafish embryos (Du et al., 2006; Just et al., 2011; Tan et al., 2006). However, in mouse embryos, *Smyd1* mRNA was restricted to the heart of mouse embryos at E10.5 with no detectable signal in the somites (Gottlieb et al., 2002). To reconcile this difference, we assayed the spatial expression of *Smyd1* mRNA in mouse embryos at E9.5 by *in situ* hybridization. In agreement with chick and zebrafish experiments, *Smyd1* mRNA was very specifically expressed in both the somites and heart (Fig. 5A). These data confirm that Smyd1 is a striated-muscle specific methyltransferase expressed within both cardiomyocyte and skeletal muscle progenitor cells.

Myf5^{cre} mice harbor an *IRES-cre* knock-in within the 5' UTR of the *Myf5* gene (Haldar et al., 2007); therefore, *cre* expression should be restricted to somitic myoblasts and absent from cardiac lineages. We confirmed this activity using the *Rosa26*^{YFP} reporter. Cre-induced recombination of *loxP* sites occurred very specifically in the somites and not in the heart (the other site of *Smyd1* expression) (Fig. 5B). These data illustrate the utility of this genetic cross to

delete *Smyd1* at the earliest stage of its expression in the skeletal muscle lineage without affecting heart development.

It was reported that the subcellular localization of Smyd1 changes during C2C12 myoblast differentiation (Berkholz et al., 2014; Sims et al., 2002); however, this has yet to be observed for endogenous Smyd1 during myogenesis *in vivo*. First, we confirmed previous reports showing export of Smyd1 from nucleus to cytosol during C2C12 differentiation. Smyd1 localized to both the nucleus and cytoplasm in undifferentiated C2C12 myoblasts (Fig. 5C). After 5 days in differentiation medium, Smyd1 localized primarily to the cytosol of myotubes (Fig. 5D). Relatively low levels of fluorescence were still detectable in the nucleus. Thus, while the majority of Smyd1 protein is cytoplasmic in myotubes, a small fraction remains in the nucleus with the potential to regulate transcription.

Next, we determined spatial and temporal expression of Smyd1 during myogenesis *in vivo*. Within the myotome at E11.5, Smyd1 and Pax7 did not co-localize (Fig. 5E-I), thus representing distinct cell populations. In contrast, Smyd1 co-localized with Myogenin (Myog) in many cells (Fig. 5J-N, white arrowheads in panel M). Individual cells could be observed expressing Myog, but little to no Smyd1 (Fig. 5M, yellow arrowheads). Cells expressing high

Smyd1 with low Myog are likely newly formed primary fibers (Fig. 5M, purple arrowheads). Similar results were observed in skeletal muscle at E16.5 (Fig. 5O-S). At this stage, Smyd1 protein is abundant in the sarcoplasm of all fibers with relatively lower levels in myonuclei. Smyd1 colocalized with Myog in many newly forming secondary fibers (Fig. 5R, white arrowheads). A small number of cells expressed Myog, but little to no Smyd1 (Fig. 5R, yellow arrowheads). Collectively, these data indicate that Smyd1 is downstream of Pax7 and Myog, being expressed in $Myog^{+}$ myoblasts, but not $Pax7^{+}$ progenitor cells.

Previous reports showed that Smyd1 localizes to the M-line of muscle fibers in zebrafish (Just et al., 2011; Li et al., 2011). Indeed by E15.5 and in adult muscle, Smyd1 exhibited a characteristic sarcomeric localization pattern with alternating bands of α-actinin and Smyd1 (Fig. 5T, U). These results are consistent with the conclusion that the majority of Smyd1 in differentiated fibers localizes to the M-line.

These data support a working model in which Smyd1 functions primarily as a nuclear transcriptional regulator during myoblast proliferation and differentiation. Later, as Smyd1 accumulates in myotube/myofiber sarcoplasm, it serves in sarcomere assembly and stability. Using *Myf5*^{cre}, we were able to deplete Smyd1 from myoblasts (Fig. 4), at a time in which the protein is most likely to be affecting the myogenic transcriptional program.

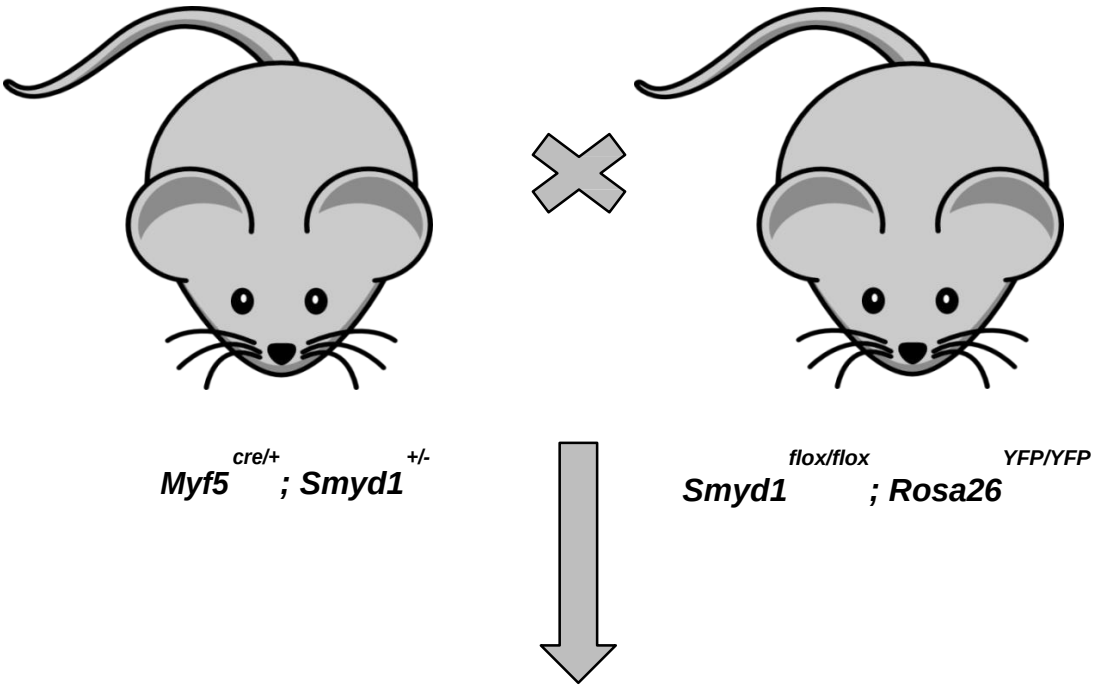

Fig. 4 Mating scheme showing mouse crossed to delete Smyd1 specifically in early muscle precursor cells (undifferentiated, proliferating muscle progenitor cells)

Fig. 5

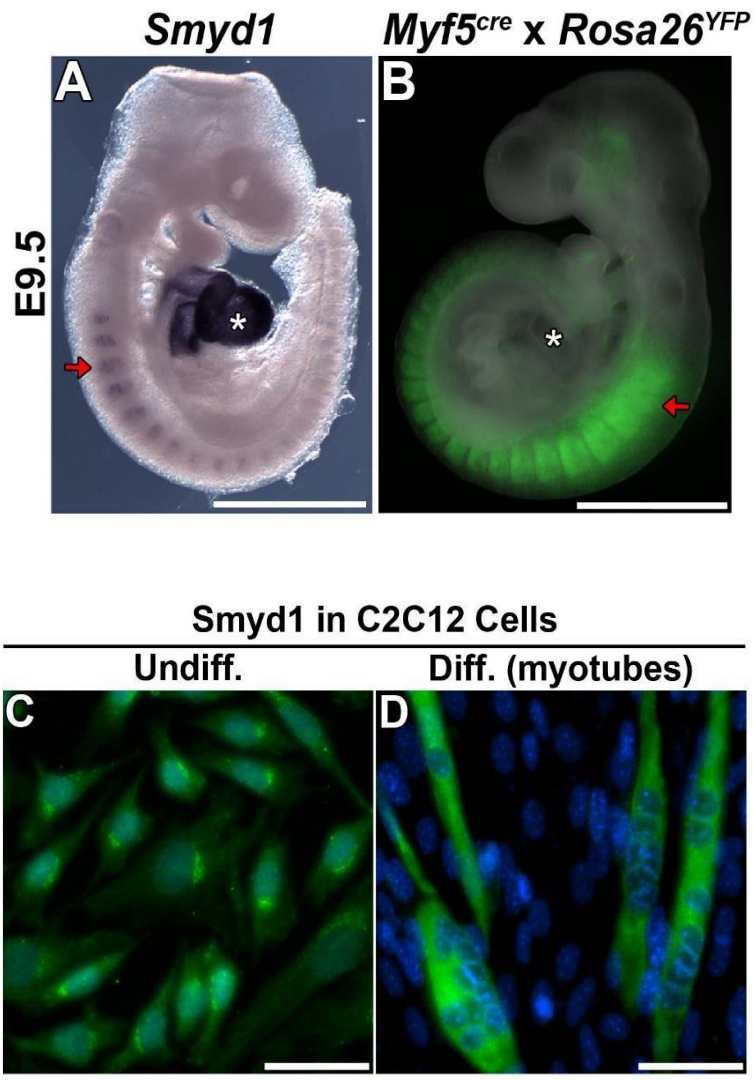

Fig. 5 Whole mount *in situ* hybridization for *Smyd1* mRNA at E9.5. *Smyd1* mRNA is specifically localized to the heart (white asterisk) and somites (red arrow) [Fig. 5A]. Stereoimage overlay of YFP fluorescence (green) and brightfield [Fig. 5B]. *Myf5*^{cre} is specifically active in the somites (red arrow), but not the heart (white asterisk) [Fig. 5B]. Immunofluorescence for Smyd1 (green) in undifferentiated C2C12 myoblasts [Fig. 5C] and myotubes after five days in differentiation medium [Fig. 5D]. Scale bars = 1 mm [Fig. 5A-B], 50 µm [Fig. 5C-D]. Ctrl, control; CKO, conditional knockout.

Fig. 5 (Continued)

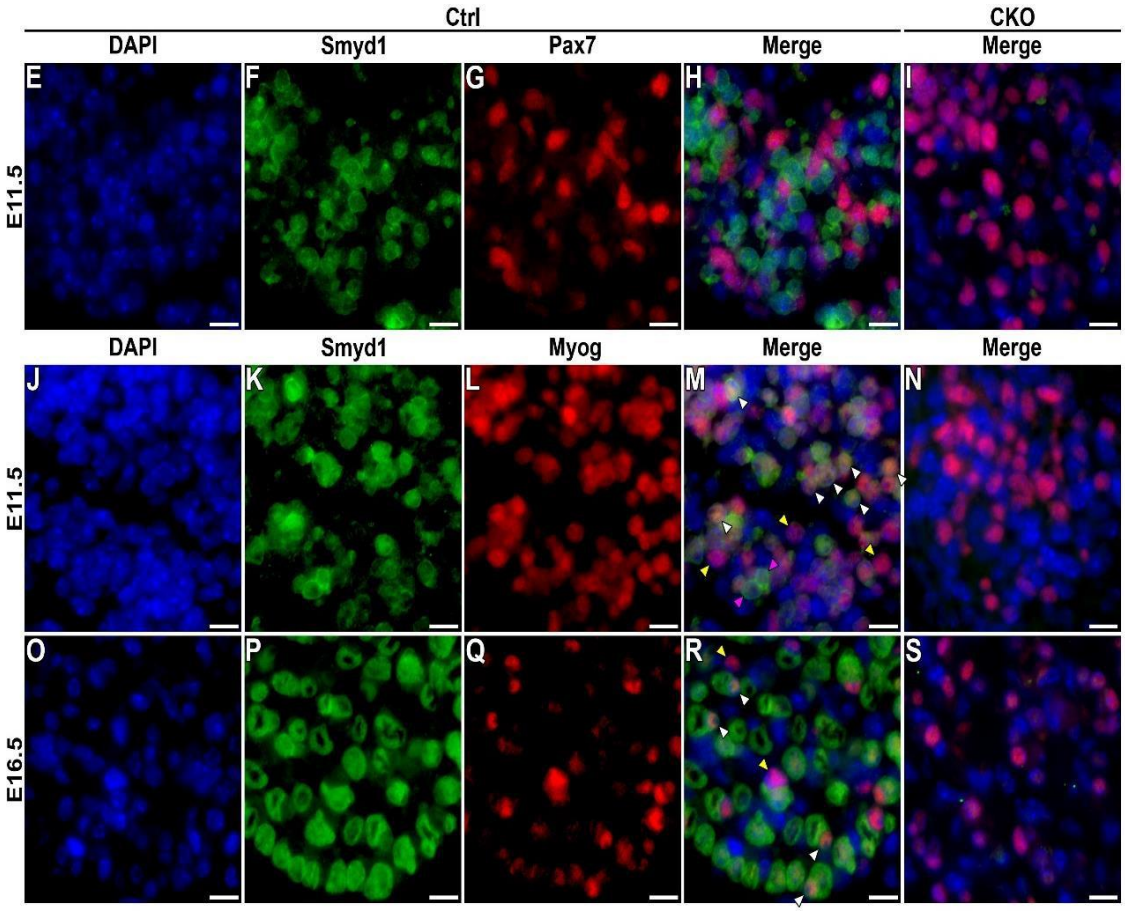

Fig. 5 (Continued) Immunofluorescence for Smyd1 (green) and Pax7 (red) in the myotome of control [Fig. 5E-H] or *Smyd1* CKO [Fig. 5I] embryos at E11.5. Immunofluorescence for Smyd1 (green) and Myog (red) in the myotome of control [Fig. 5J-M] or *Smyd1* CKO [Fig. 5N] embryos at E11.5. Immunofluorescence for Smyd1 (green) and Myog (red) in the EDL muscle of control [Fig. 5O-R] or *Smyd1* CKO [Fig. 5S] embryos at E16.5. White arrowheads, co-localization of Smyd1 and Myog; yellow arrowheads, $Myog^{+}$ $Smyd1^{-}$ cells; purple arrowheads, young fibers with low Myog and high Smyd1 [Fig. 5M,R]. Scale bar = 10 μm [Fig. 5E-S]. Ctrl, control; CKO, conditional knockout.

Fig. 5 (Continued)

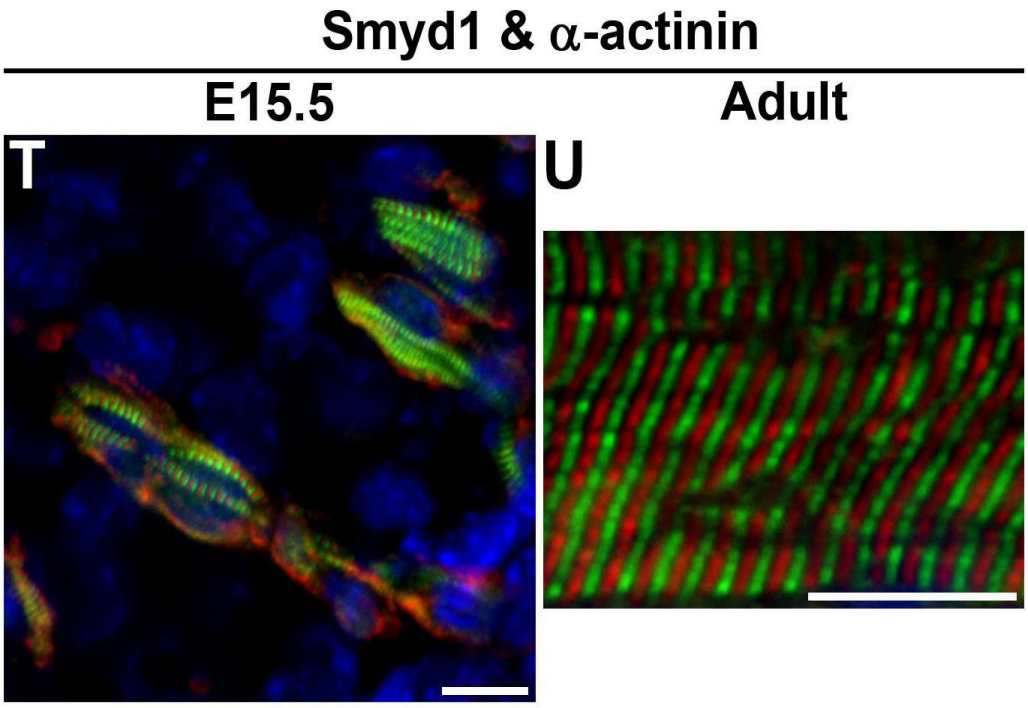

Fig. 5 (Continued) Immunofluorescence for Smyd1 (green) and α-actinin (red) in longitudinal skeletal muscle sections of wild-type embryos at E15.5 [Fig. 5T] and adult soleus muscle [Fig. 5U]. Blue, nuclei (DAPI). Scale bar = 10 μm [Fig. 5T-U]. Ctrl, control; CKO, conditional knockout.

Smyd1 CKO embryos appear normal during the first wave of myogenesis.

At E11.5, during the first wave of myogenesis, *Smyd1* CKO embryos were indistinguishable from control embryos (Fig. 6A, B). *In situ* hybridization for *α-actin* showed normal somitogenesis in *Smyd1* CKOs at E10.5 (Fig. 6C), with no difference in myotome width between controls and CKOs (Fig. 6D). In order to confirm Smyd1 deletion during the first myogenic wave at E11.5, transverse sections from control and Smyd1 CKO embryos were immuno-stained for Smyd1. While the myotomal regions in control embryo sections showed Smyd1 expression in the nucleus and cytoplasmic compartments (Fig. 6E-F), there was barely any Smyd1 detected in the Smyd1 CKO sections (Fig. 6G-H), hence showing efficient deletion of Smyd1 at this stage. The next test was to examine whether loss of *Smyd1* affected muscle gene expression during the first wave of myogenesis. At E11.5, the midpoint of the first wave, mRNA expression of major transcription factors regulating skeletal myogenesis program (*Pax3, Pax7, Myf5, Myod1, Myog,* and *Myf6*) was equivalent between control and CKO embryos (Fig. 6Q-T). At the same stage, mRNA expression of several skeletal muscle specific markers (*Acta1* (α-actin)*, Myh3* (embryonic MyHC)*, Myh7* (slow MyHC)*, Myh8* (Fetal MyHC)*, Ckm* (creatine kinase) and *Eno3* (β-enolase)) was also equivalent (Fig. 6M-P). These data point to normal initiation of the skeletal myogenesis program in the absence of Smyd1.

Fig. 6A

Control

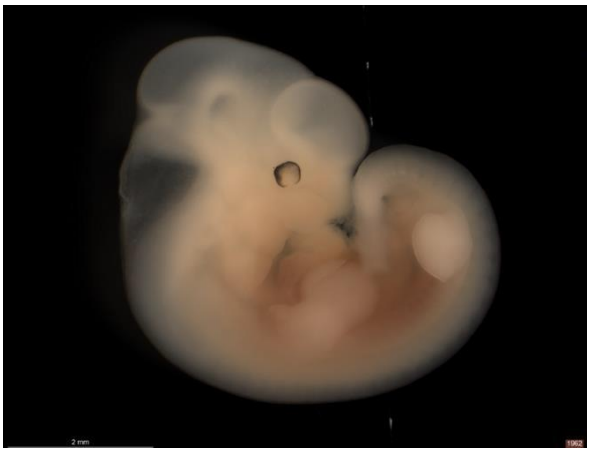

Fig. 6B

CKO

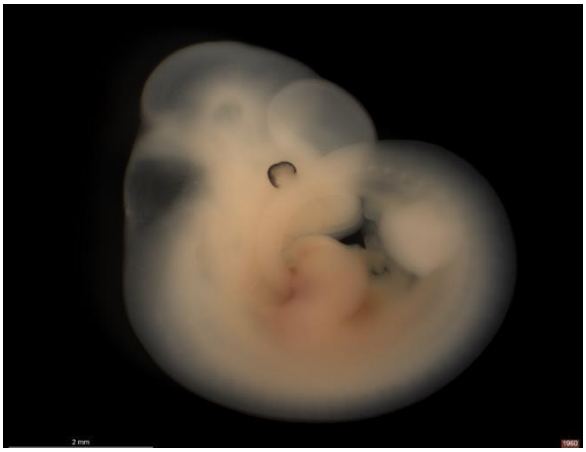

Fig. 6 Stereo images of [Fig. 6A] Control and [Fig. 6B] Smyd1-myf5cre-CKO embryos at E11.5 during the first myogenic wave. Scale bar = 1mm [Fig. 6A-B]. Ctrl, control; CKO, conditional knockout.

Fig. 6C (Fig. 6 Continued)

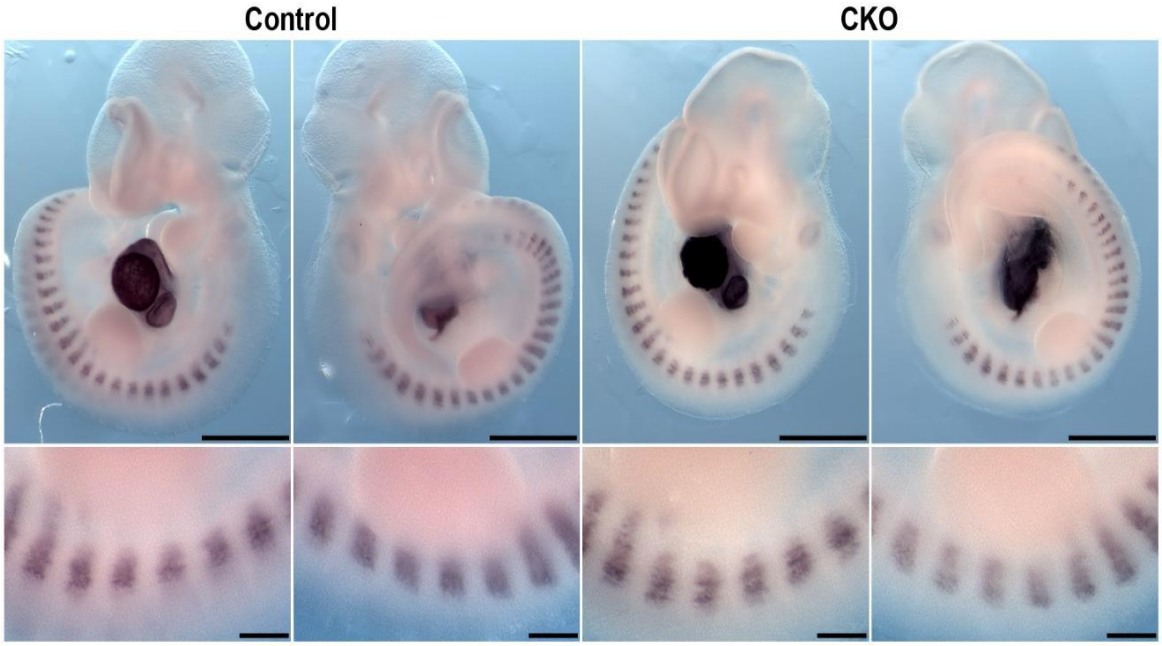

Fig. 6D

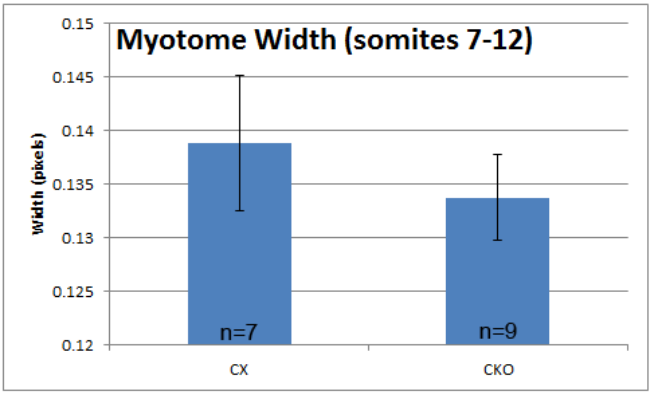

Fig. 6 (Continued) Insitu hybridization for α-actin at E10.5 using control and Smyd1-myf5cre-CKO embryos [Fig. 6C] shows no difference in myotome width during the first wave of myogenesis upon subsequent quantification [Fig. 6D]. For full embryo figures, scale bar = 1mm and for figures showing somites in detail, scale bar =0.2 mm. CKO, conditional knockout

Fig. 6 (Continued)

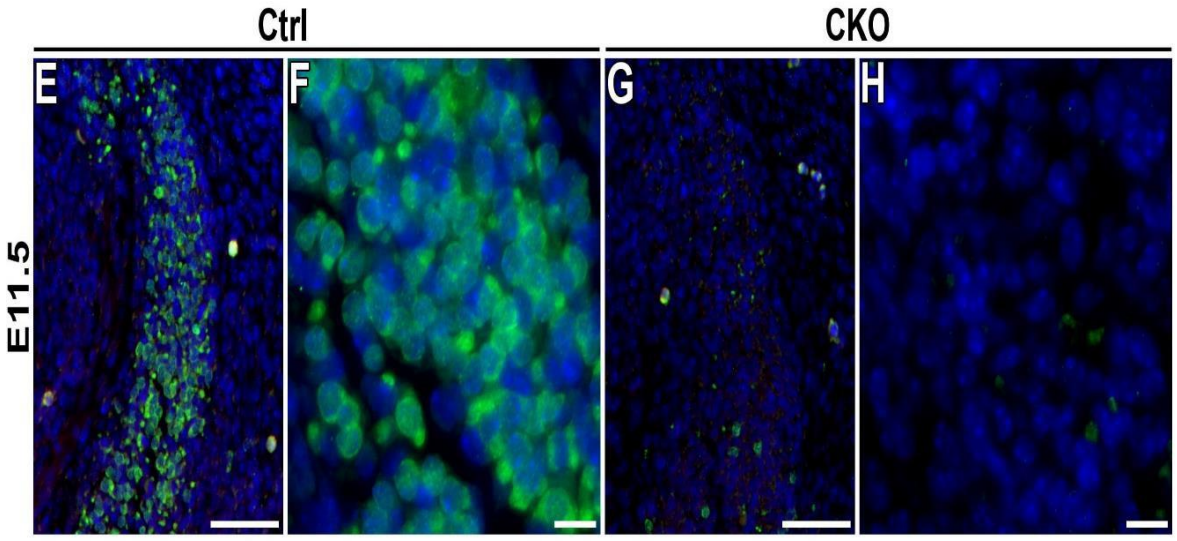

Fig. 6 (Continued) Immuno-fluorescence for Smyd1 (green) and nuclei (blue) at E11.5 highlights myotome in control embryo [Fig. 6E-F] and validates Smyd1 deletion in Smyd1-myf5cre-CKO embryos [Fig. 6G-H] at E11.5 during the first myogenic wave. Fig. 6F and Fig. 6H show a portion of Fig. 6E & 6G at higher magnification respectively. Scale bar = 50 um [Fig. 6E & 6G]; 10 um [Fig. 6F & 6H]. Ctrl, control; CKO, conditional knockout.

Fig. 6 (Continued)

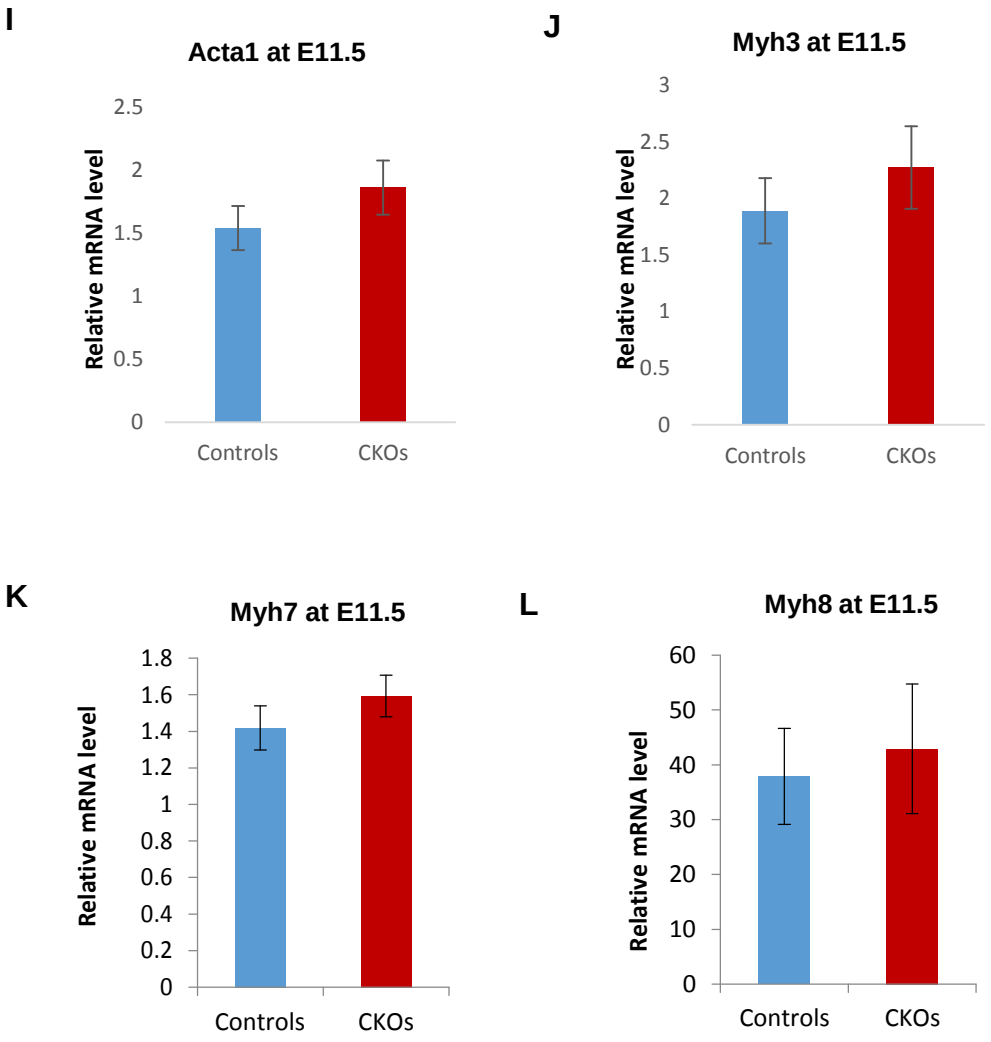

Fig. 6 (Continued) qPCR for skeletal muscle specific genes at E11.5 shows no difference in relative mRNA levels between controls and Smyd1 CKOs [Fig. 6I-L]. *****P < 0.05, ******P < 0.01, *******P < 0.001, Student's *t* test. CKO - Conditional knock-out.

Fig. 6 (Continued)

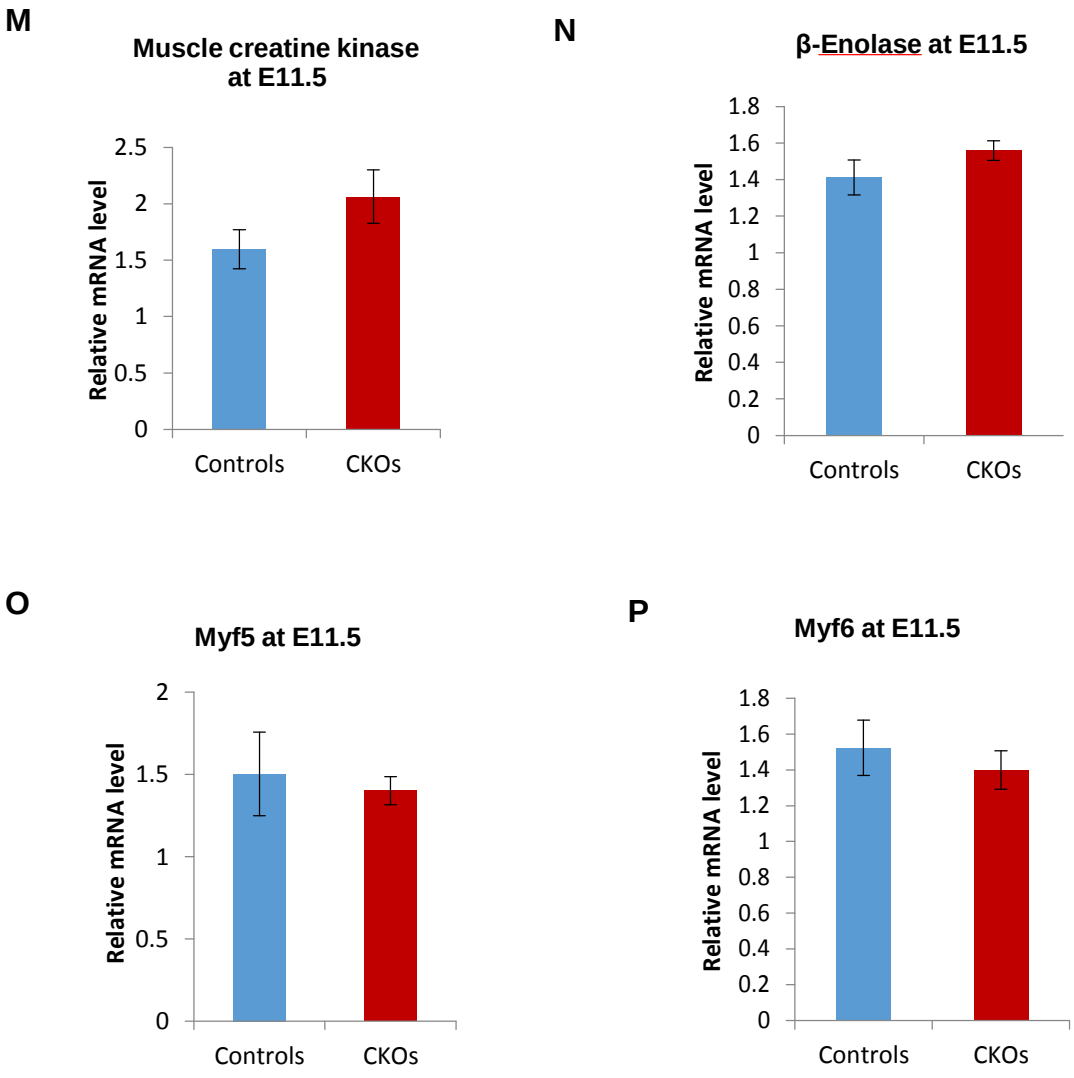

Fig. 6 (Continued) qPCR for skeletal muscle specific genes at E11.5 shows no difference in relative mRNA levels between controls and Smyd1 CKOs [Fig. 6M-P]. *****P < 0.05, ******P < 0.01, *******P < 0.001, Student's *t* test. CKO - Conditional knock-out.

Fig. 6 (Continued)

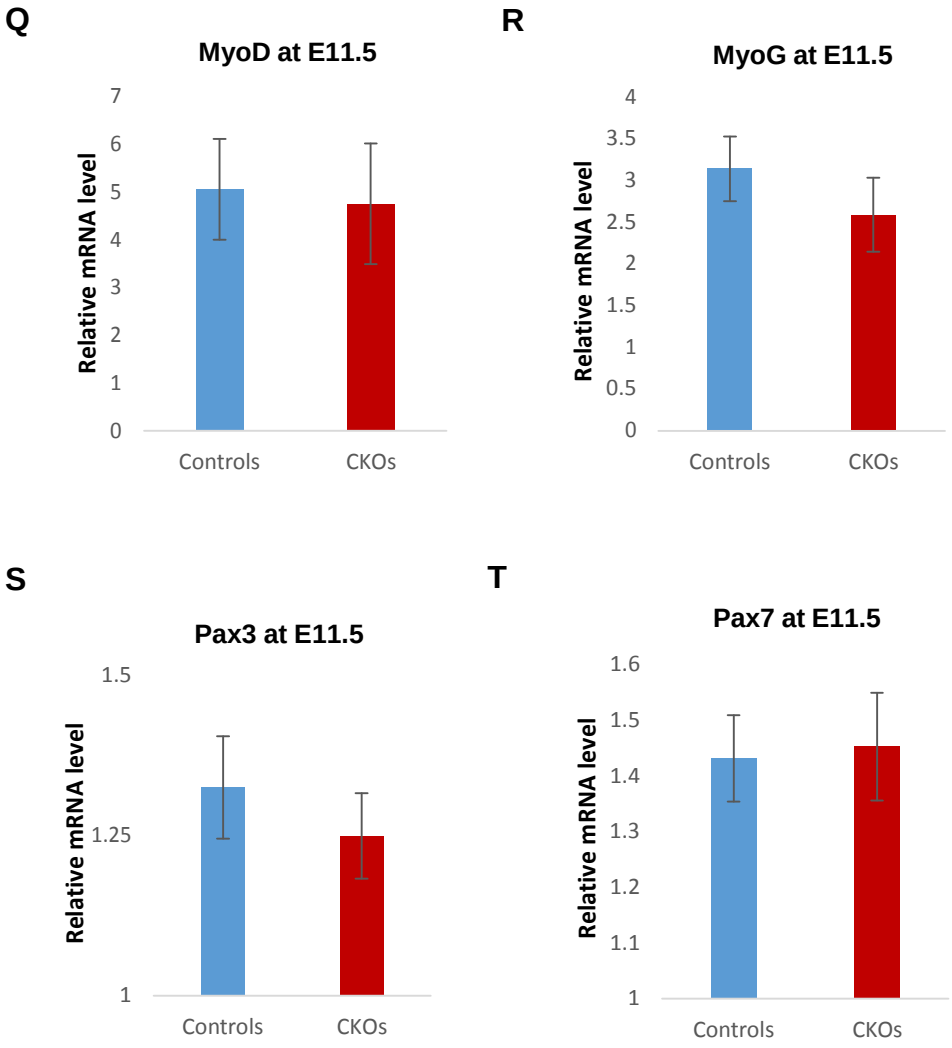

Fig. 6 (Continued) qPCR for skeletal muscle specific genes at E11.5 shows no difference in relative mRNA levels between controls and Smyd1 CKOs [Fig.6Q-T]. *****P < 0.05, ******P < 0.01, *******P < 0.001, Student's *t* test. CKO - Conditional knock-out.

Table-1 Summary of qPCR results for muscle specific genes during the first wave of myogenesis at E11.5

Gene	Description	Statistically significant difference between control and Smyd1-myf5cre-CKO embryos at E11.5?
Pax3	One of the earliest transcription factor expressed during skeletal myogenesis. Marker for muscle precursor cells	No
Pax7	Transcription factor that acts downstream of Pax3. Also a marker for muscle precursor cells	No
Myf5	Myogenic regulatory factor (MRF) involved in myoblast specification. Acts downstream of Pax3 and Pax7	No
MyoD	Myogenic regulatory factor (MRF) involved in myoblast specification. Acts downstream of Pax3 and Pax7	No
MyoG	MRF that acts downstream of Myf5 and MyoD, involved in differentiation of myoblasts to myocytes	No
Myf6	MRF that acts downstream of MyoG, involved in terminal differentiation of myotubes/myofibers	No

Table -1 (Continued)

Gene	Description	Statistically significant difference between control and Smyd1-myf5cre-CKO embryos at E11.5?
Acta1	Major component of sarcomere (skeletal actin)	No
Myh3	Fetal myosin heavy chain (cytoskeletal protein)	No
Myh7	Myosin heavy chain specific to slow twitch muscle fibers	No
Myh8	Myosin heavy chain specific to fast twitch muscle fibers	No
Mck	Muscle creatine kinase, enzyme involved in energy homeostasis	No
Beta-enolase	Skeletal muscle specific enzyme, catalyzes final step of glycolysis	No

Fig. 7

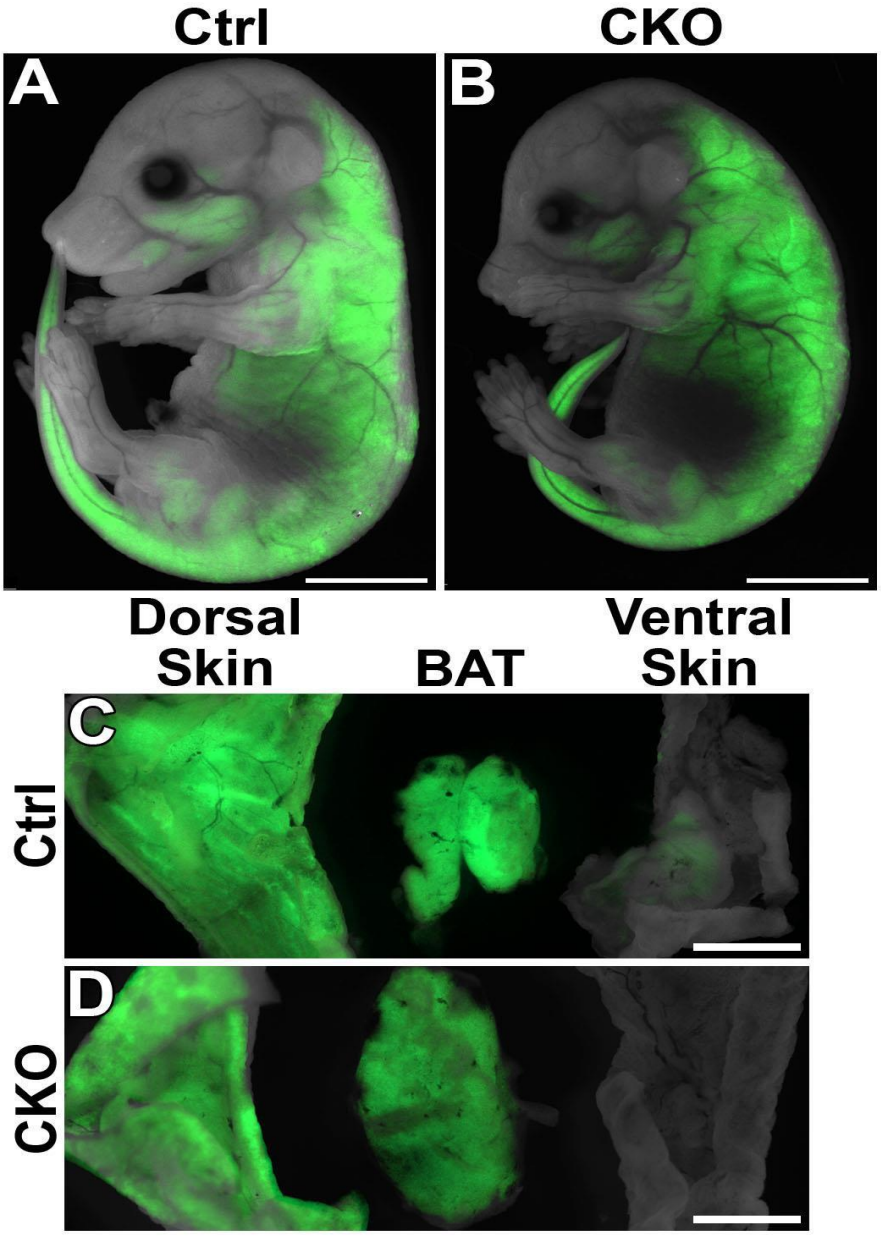

Fig. 7 Overlay of YFP (green) and brightfield stereo-fluorescence images at E15.5 showing *Myf5*^{cre} fate map. *Myf5* lineage cells are similarly distributed in skeletal muscles, tail and dorsal tissues of both control [Fig. 7A] and *Smyd1* CKO [Fig. 7B] embryos. *Myf5*$^{+}$ cells give rise to dorsal skin and brown adipose, but not ventral skin in both control [Fig. 7C] and *Smyd1* CKO [Fig. 7D] embryos. Scale bar = 2mm [Fig. 7A-D]. Ctrl, control; CKO, conditional knockout.

Smyd1 CKO embryos exhibit reduced muscle mass and subcutaneous edema during the second myogenic wave. *Myf5*^{cre}-induced recombination was restricted to the skeletal muscle lineage, dorsal epidermis and brown adipose of control and *Smyd1* CKO embryos as determined by fluorescence from the *Rosa26*^{YFP} reporter (Fig. 7A-D). Loss of Smyd1 protein was confirmed by western blot using protein extracts from the body wall of E16.5 embryos (Fig. 7E). By E15.5, *Smyd1* CKO embryos were easily distinguished from control littermates by dorsal subcutaneous edema (Fig. 7F, G). Transverse tissue sections were prepared at the level of the forelimbs for H&E staining and immunofluorescence. In these sections, the dorsal subcutaneous edema manifested as a wide region of loose connective tissue between the skin and back muscles (Fig. 7H, I). This pathology may be similar to the "amorphous connective tissue" reported in *Myf5/MyoD* double knockout mice, which completely lack skeletal muscle (Rudnicki et al., 1993). Back muscles also appeared diminished in H&E sections (Fig. 7H, I). Relative muscle mass was compared between control and *Smyd1* CKO embryos by immunofluorescence for sarcomeric α-actinin. Far less α-actinin staining was observed in *Smyd1* CKO embryos (Fig. 7J, K). Furthermore, in western blots, *Smyd1* CKO embryos exhibited less total myosin heavy chain protein than controls (Fig. 7E). These data indicate reduced muscle mass during the second wave of myogenesis in the absence of Smyd1.

Fig. 7 (Continued)

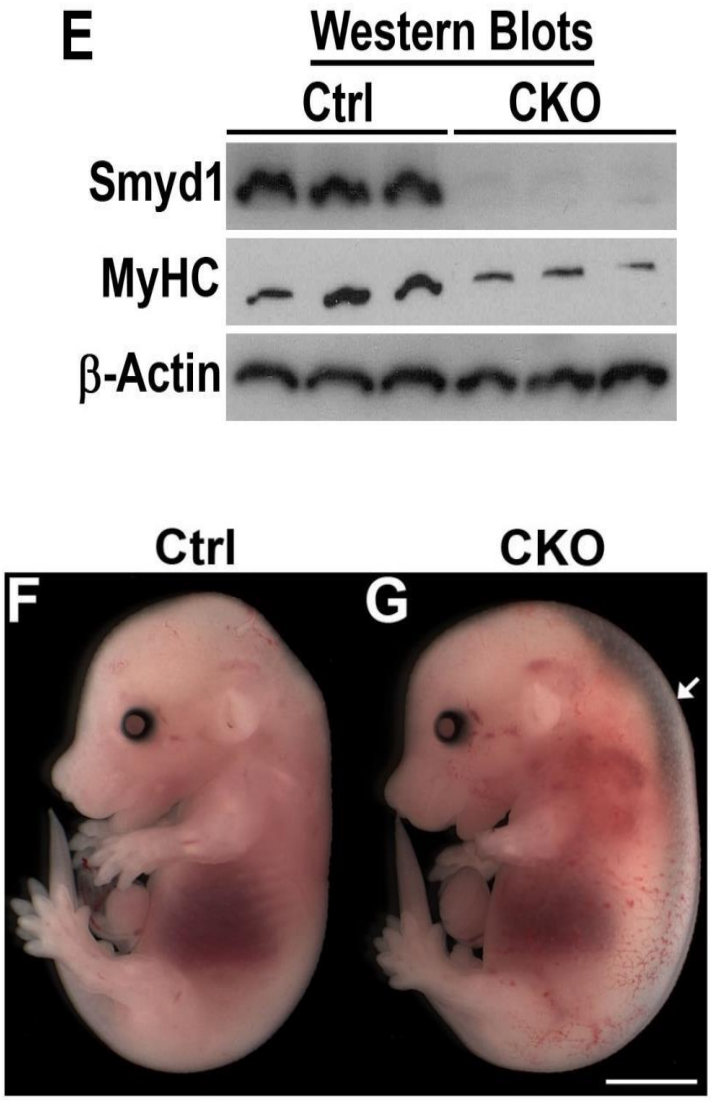

Fig. 7 (Continued) Western blots using body wall extracts from E16.5 embryos. Smyd1 protein was undetectable in *Smyd1* CKO embryos [Fig. 7E]. Total myosin heavy chain (MyHC) was reduced in *Smyd1* CKO embryos [Fig. 7E]. Anti-β-actin was used as a loading control. Brightfield stereo images at E15.5 [Fig. 7F-G]. *Smyd1* CKO embryos exhibit subcutaneous edema (white arrow) [Fig. 7G] across the length of the dorsal side. Scale bar = 2mm. Ctrl, control; CKO, conditional knockout.

Fig. 7 (Continued)

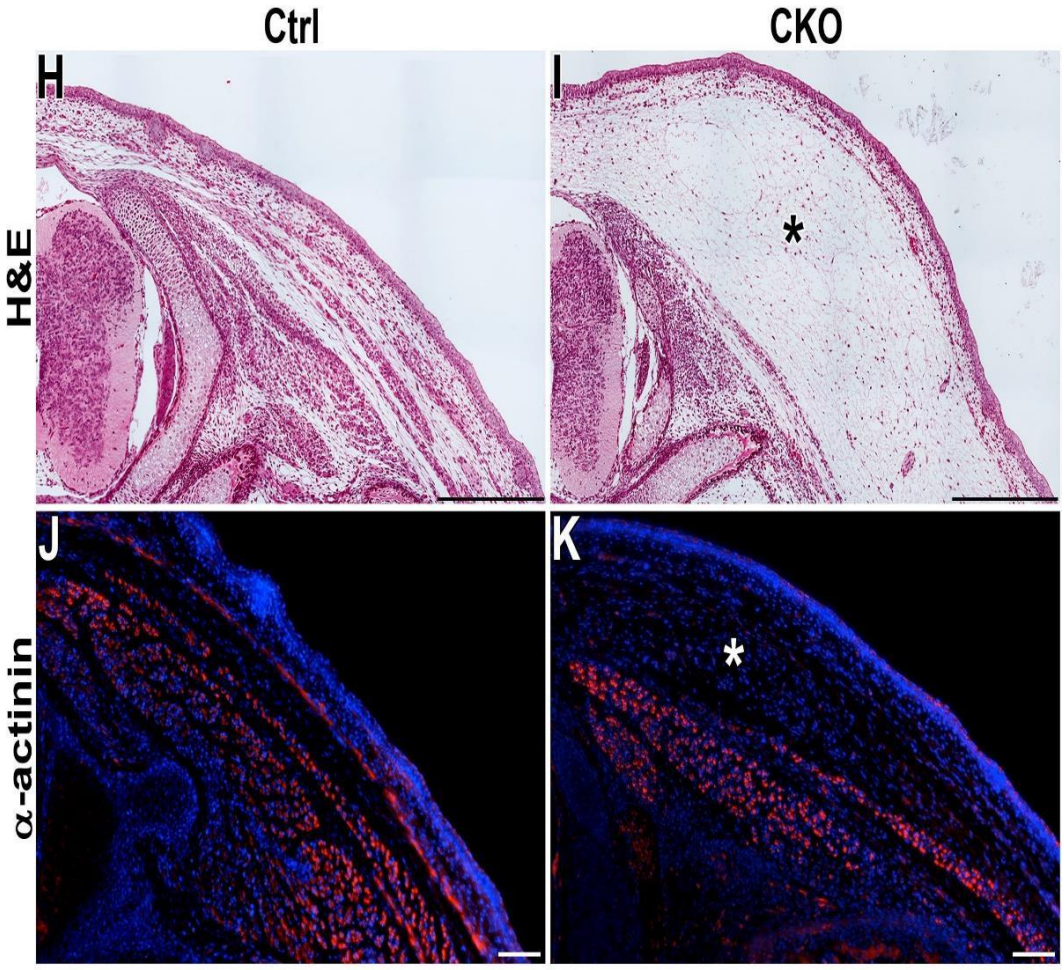

Fig. 7 (Continued) H&E-stained transverse sections (dorsal quarter) at E15.5 [Fig. 7H-I]. A region of subcutaneous expanded loose connective tissue (black asterisk) is prominent in *Smyd1* CKO embryos [Fig. 7I&K]. Immunofluorescence for α-actinin (red) [Fig. 7J-K] showing reduced abundance of myofibers in *Smyd1* CKO embryos at E15.5. Blue, nuclei (DAPI). Asterisk, subcutaneous edema. Scale bars = 500 µm [Fig. 7H-I]; 100 µm [Fig. 7J-K]. BAT, brown adipose tissue; Ctrl, control; CKO, conditional knockout; MyHC, myosin heavy chain.

Fewer muscle fibers and reduced muscle gene expression during the second wave of myogenesis. Myofiber abundance and organization was assayed by immunofluorescence using a pan-myosin antibody (MF-20). Longitudinal sections of tibialis anterior (TA) and extensor digitorum longus (EDL) muscles at E16.5 showed disorganized arrangement of muscle fibers in *Smyd1* CKOs (Fig. 8A, B). Similarly stained transverse sections of TA and EDL muscles revealed less densely packed muscle fibers in *Smyd1* CKOs (Fig. 8C, D). The abundance of primary and secondary myofibers was quantified in transverse EDL sections immuno-labelled for myosin heavy chain (such as those illustrated in Fig. 8C, D). Two sections each from nine *Smyd1* CKO and ten control embryos were used for counting. The data was normalized to the cross-sectional area of the muscle. *Smyd1* CKOs exhibited significantly fewer primary and secondary fibers as compared to the controls during the second wave of myogenesis (Fig. 8E, F). Percentagewise, secondary fiber development was impaired more than primary fiber development.

Our next experiment was to test if the reduction in myofibers was due to alterations in expression of myogenic transcription factors. Real-time PCR at E15.5 showed *Pax3*, which exhibits relatively higher expression in embryonic myoblasts and myotubes than in fetal myoblasts and myotubes (Biressi et al., 2007b), was elevated in the *Smyd1* CKO. *Pax7*, *Myod1* and *Myog* were

unaffected; *Myf5* and *Myf6* were down regulated (Fig. 8P-S, N-O). Expression of genes associated with differentiated skeletal myocytes was next examined. mRNA levels of *Acta1* (α-actin), *Myh3* (embryonic MyHC), *Myh7* (slow MyHC), *Myh8* (fetal MyHC), *Ckm* (muscle creatine kinase) and *Eno3* (β-enolase) were reduced in the *Smyd1* CKO at E15.5 (Fig. 8H-K). These results indicate loss of *Smyd1* impairs myofiber development during the second myogenic wave and support our observation of fewer muscle fibers in the *Smyd1* CKOs at E16.5.

Since reduced myofiber abundance might result from myofiber degeneration, width of the myosin ring surrounding nuclei of primary fibers and expression of atrophy-associated genes *Trim63/Murf1* and *Fbxo32/MAFbx/Atrogin1* was measured. There was no difference in myofiber width (Fig. 8G) nor in expression of *Trim63* or *Fbxo32* (Table-2). These data indicate that reduced myofiber abundance was not due to degeneration.

Fig. 8

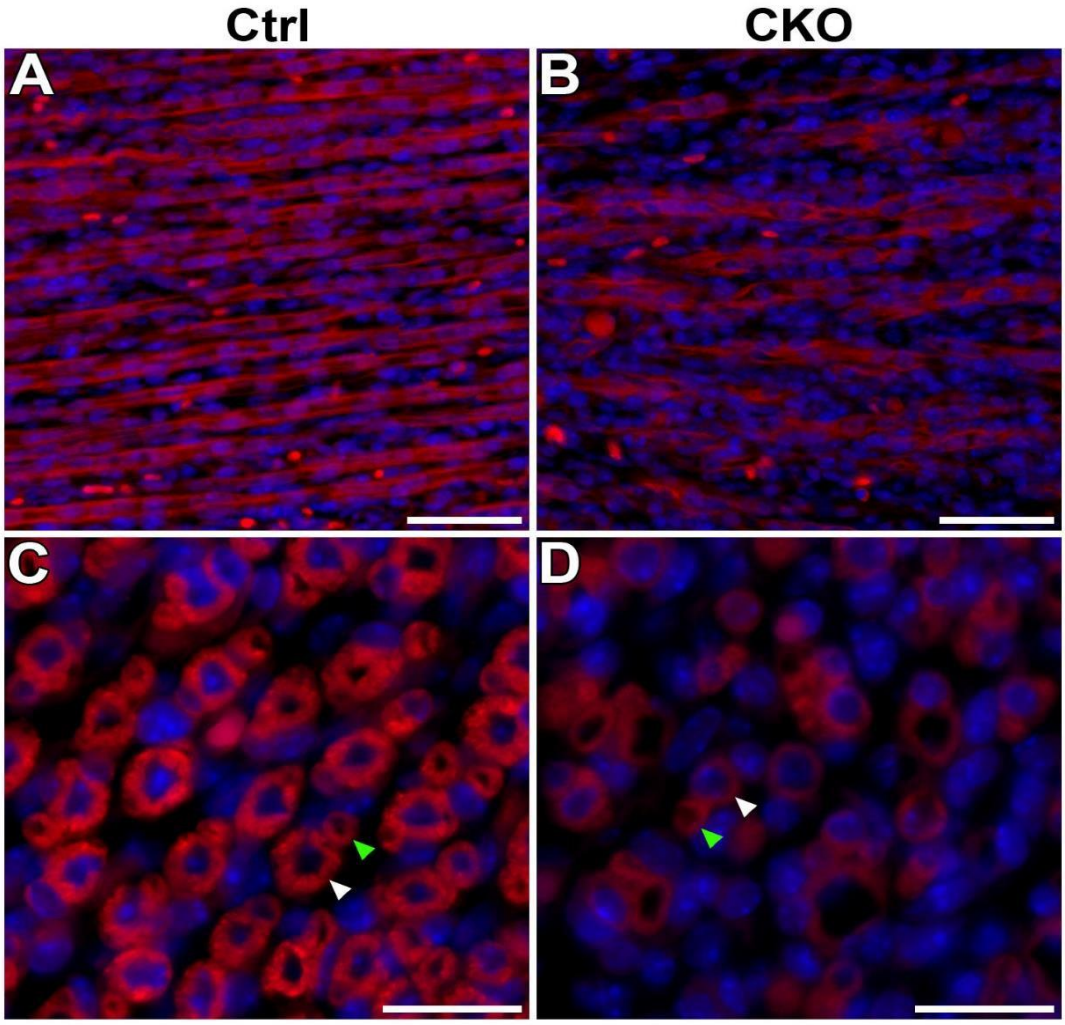

Fig. 8 Immunofluorescence for myosin heavy chain (red) in longitudinal [Fig. 8A-B] and transverse [Fig. 8C-D] sections of the EDL muscle at E16.5. Blue, nuclei (DAPI). Scale bar = 50 um [Fig. 8A-D]. Ctrl, control; CKO, conditional knockout.

Fig. 8 (Continued)

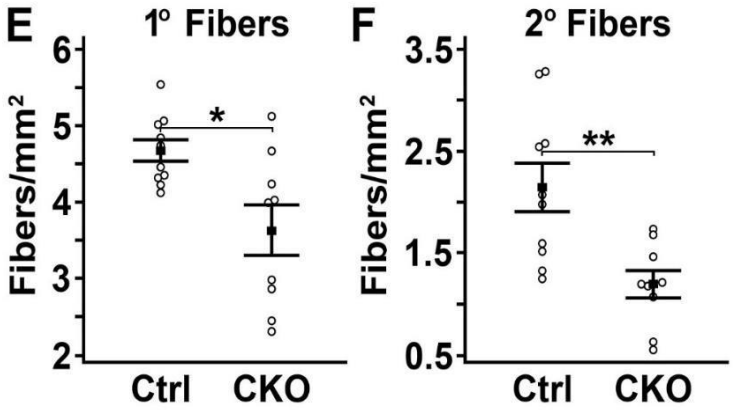

G Primary fibers

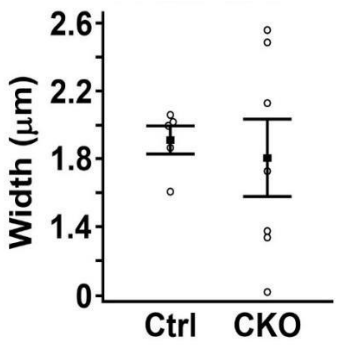

Fig. 8 (Continued) Quantification of the number of primary [Fig. 8E] and secondary [Fig. 8F] myofibers in the EDL. *Smyd1* CKO EDL exhibited less primary and secondary fibers than controls ($n \geq 9$ embryos/group). Thickness of myosin ring surrounding nuclei of primary fibers [Fig. 8G]. No difference was observed ($n \geq 5$ embryos/group). *P < 0.05, **P < 0.01, Student's *t* test. Error bars indicate SEM. Ctrl, control; CKO, conditional knockout.

Fig. 8 (Continued)

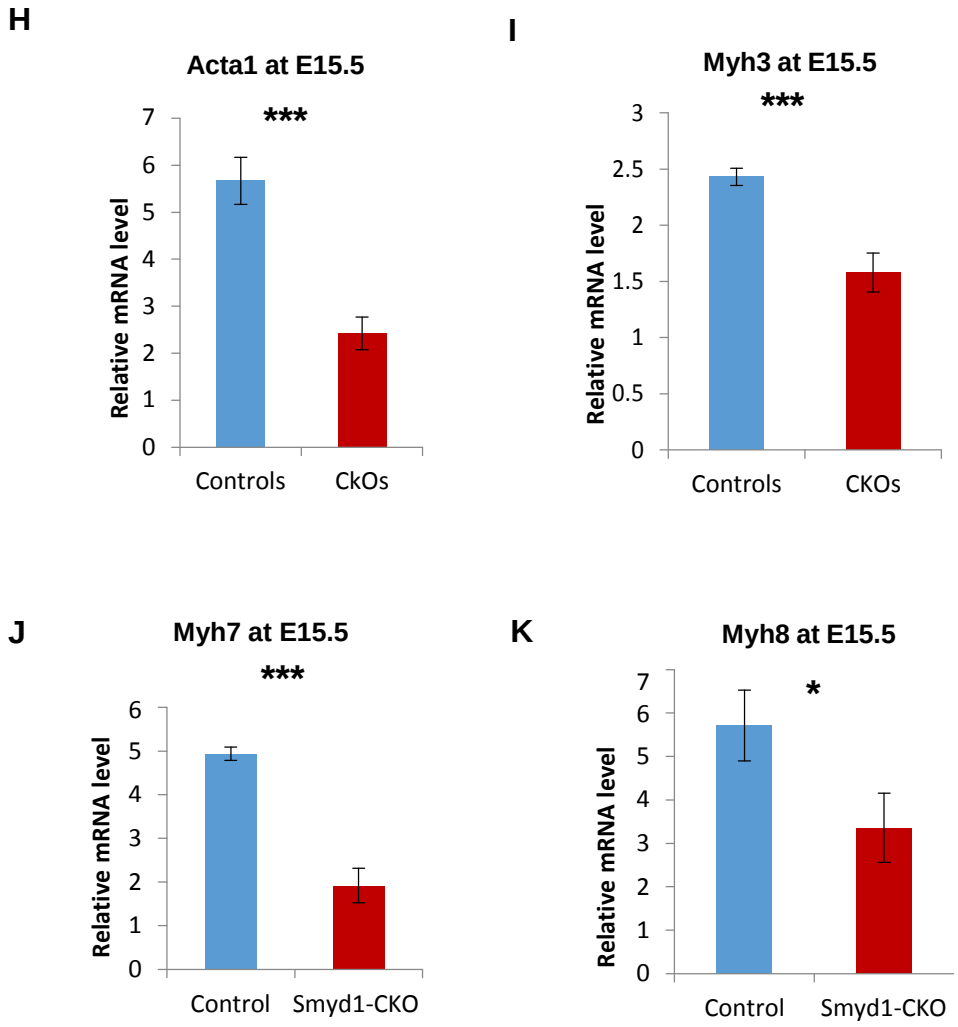

Fig. 8 (Continued) qPCR at E15.5 revealed significant down-regulation in relative mRNA levels of skeletal muscle specific genes in Smyd1 CKOs as compared to control embryos [Fig. 8H-K]. *P < 0.05, **P < 0.01, ***P < 0.001, Student's *t* test. CKO - Conditional knock-out.

Fig. 8 (Continued)

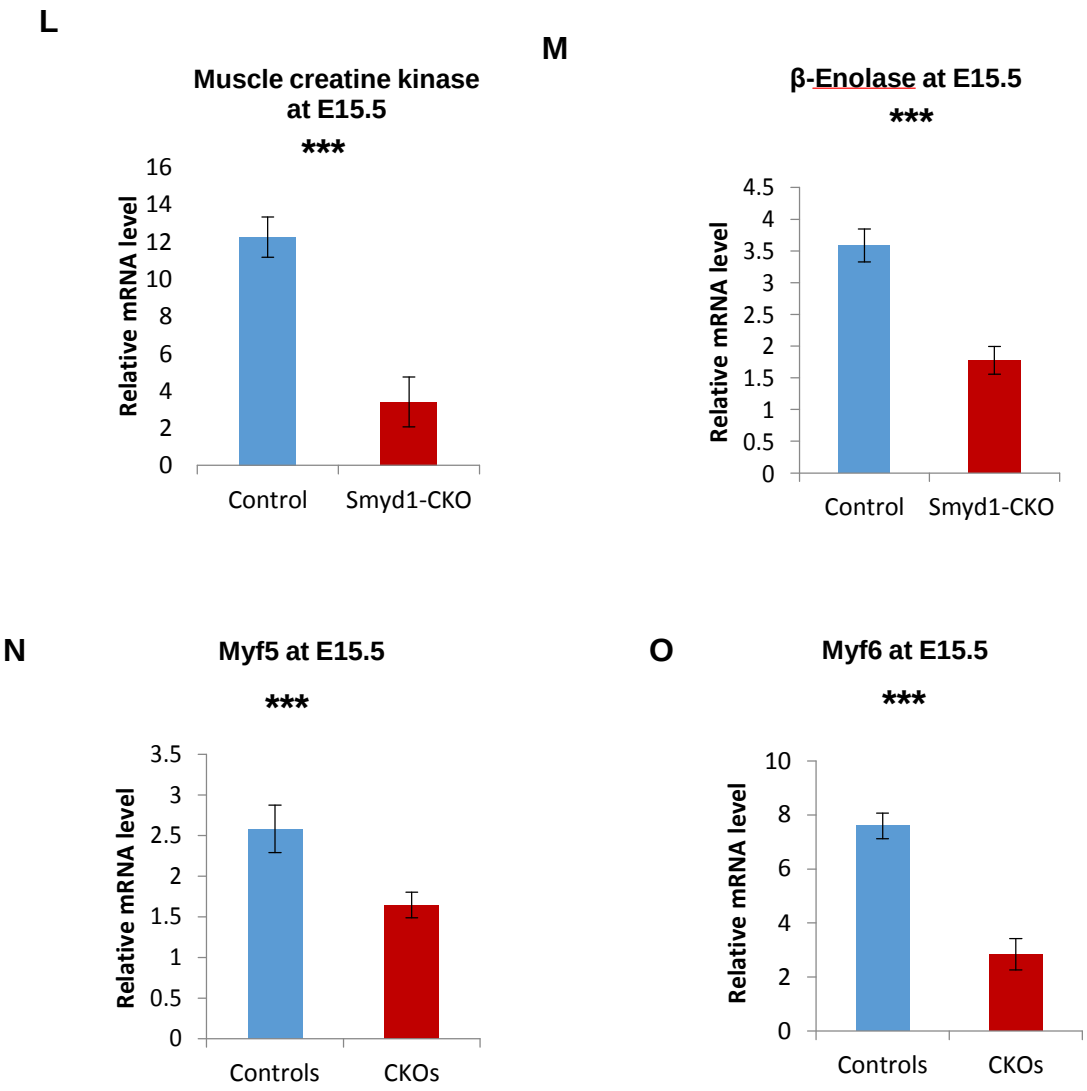

Fig. 8 (Continued) qPCR at E15.5 revealed significant down-regulation in relative mRNA levels of skeletal muscle specific genes in Smyd1 CKOs as compared to control embryos [Fig. 8L-O]. *P < 0.05, **P < 0.01, ***P < 0.001, Student's *t* test. CKO - Conditional knock-out.

Fig. 8 (Continued)

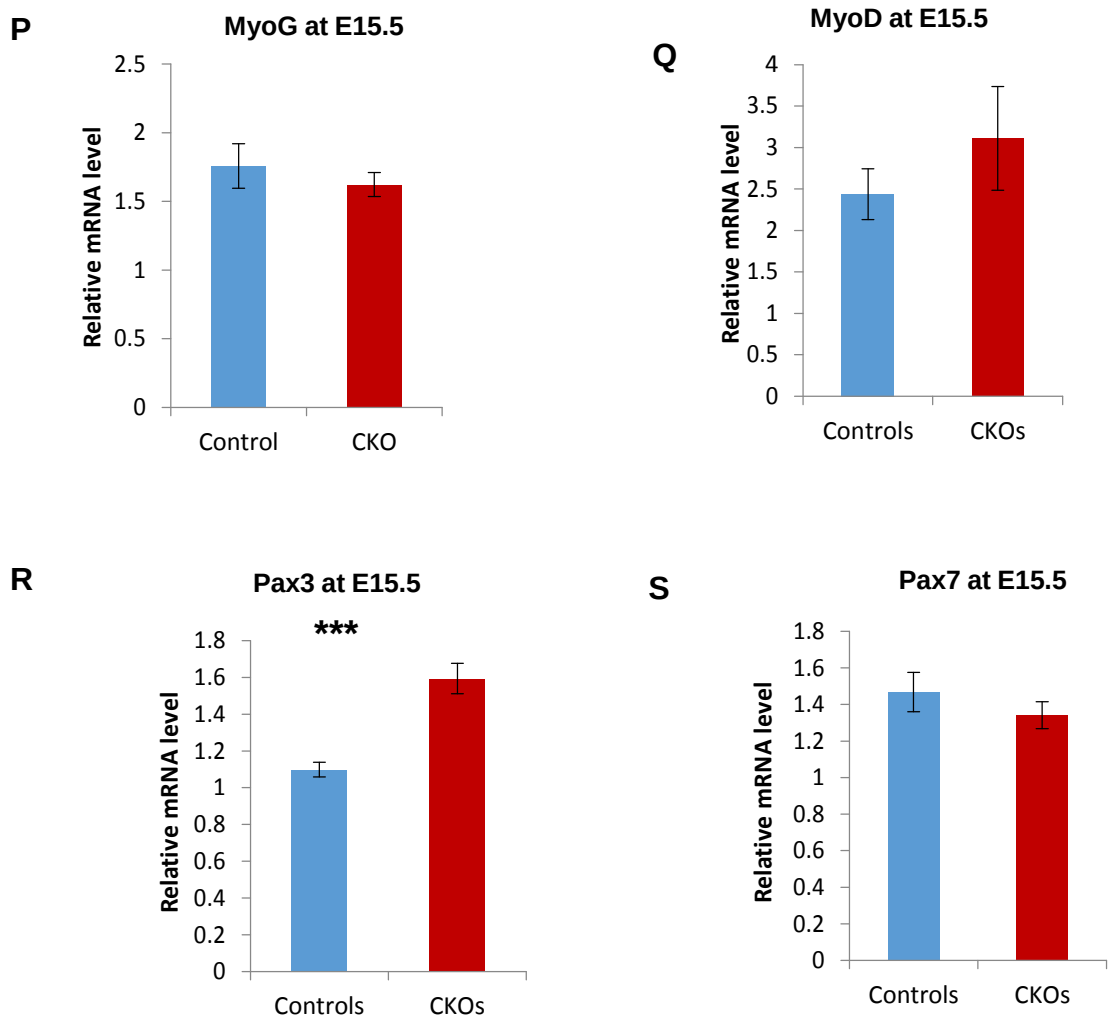

Fig. 8 (Continued) qPCR at E15.5 revealed significant down-regulation in relative mRNA levels of skeletal muscle specific genes in Smyd1 CKOs as compared to control embryos [Fig. 8P-S]. *****P < 0.05, ******P < 0.01, *******P < 0.001, Student's *t* test. CKO - Conditional knock-out.

Table-2 Summary of qPCR results for muscle specific genes during the second wave of myogenesis at E15.5. *****P < 0.05, ******P < 0.01, *******P < 0.001, Student's *t* test. CKO - Conditional knock-out.

Gene	Description	Statistically significant difference between control and Smyd1-myf5cre-CKO embryos at E15.5?
Pax3	One of the earliest transcription factor expressed during skeletal myogenesis. Marker for muscle precursor cells	Up-regulation in CKOs ***
Pax7	Transcription factor that acts downstream of Pax3. Also a marker for muscle precursor cells	No
Myf5	Myogenic regulatory factor (MRF) involved in myoblast specification. Acts downstream of Pax3 and Pax7	Down-regulation in CKOs ***
MyoD	Myogenic regulatory factor (MRF) involved in myoblast specification. Acts downstream of Pax3 and Pax7	No
MyoG	MRF that acts downstream of Myf5 and MyoD, involved in differentiation of myoblasts to myocytes	No

Table -2 (Continued) Gene	Description	Statistically significant difference between control and Smyd1-myf5cre-CKO embryos at E15.5?
Myf6	MRF that acts downstream of MyoG, involved in terminal differentiation of myotubes/myofibers	Down-regulation in CKOs ***
Acta1	Major component of sarcomere (skeletal actin)	Down-regulation in CKOs ***
Myh3	Fetal myosin heavy chain (cytoskeletal protein)	Down-regulation in CKOs ***
Myh7	Myosin heavy chain specific to slow twitch muscle fibers	Down-regulation in CKOs ***
Myh8	Myosin heavy chain specific to fast twitch muscle fibers	Down-regulation in CKOs *
Mck	Muscle creatine kinase, enzyme involved in energy homeostasis	Down-regulation in CKOs ***
Beta-enolase	Skeletal muscle specific enzyme, catalyzes final step of glycolysis	Down-regulation in CKOs ***
Trim63/Murf1	Atrophy associated gene	No
Fbxo32/MAFbx/Atrogin1	Atrophy associated gene	No

Loss of Smyd1 impairs myoblast differentiation. Next, we tested whether the reduction in myofibers was due to alterations in myoblast proliferation, differentiation or induced cell death. Transverse sections of E11.5 embryos at the depth of the forelimb bud were immuno-stained for Pax7. The myotomes of control and *Smyd1* CKO embryos displayed equivalent abundance of $Pax7^+$ cells (Fig. 9A, B). The number of $Pax7^+$ cells were counted and normalized with respect to t9otal myotome nuclei. We found no difference in the number of Pax7 expressing myoblasts between control and *Smyd1* CKO embryos during the first wave of myogenesis (Fig. 9C). At E15.5, during the second wave of myogenesis, we performed a similar experiment using transverse sections of EDL muscles. Again, we observed no difference in the abundance of $Pax7^+$ cells within EDL cross-sections (Fig. 9D, E). Quantification of the percentage of $Pax7^+$ cells confirmed that conclusion (Fig. 9F). However, comparison of the total number of myofibers relative to the number of $Pax7^+$ cells indicated that fewer myofibers arose from approximately the same number of $Pax7^+$ myogenic progenitor cells in the *Smyd1* CKO (Fig. 9G). We next utilized expression of YFP from the $Rosa26^{YFP}$ allele to compare the number of myofibers relative to non-myofiber *Myf5* lineage cells (myoblasts) in EDL cross-sections (Fig. 9H, I). We found a significant decrease in the number of myofibers per myoblast (Fig. 9J).

To determine if the observed reduction in *Smyd1* CKO myofiber density resulted from a myoblast proliferation defect, pregnant mice carrying E15.5 embryos were administered BrdU four hours prior to sacrifice. Proliferating myoblasts were identified by co-localization of BrdU and YFP in cross-sections of EDL muscle (Fig. 9K, L), and quantified as the percentage of total nuclei within the EDL (Fig. 9M). We observed no significant difference in proliferation rates between control and *Smyd1* CKO myoblasts. We then tested the most likely alternative explanation, apoptosis. TUNEL assays using E15.5 EDL cross-sections, however, identified very few (1-2/section) apoptotic cells in either control or *Smyd1* CKO embryos (Fig. 9N, O). In sum, we found reduced myofiber abundance in the presence of comparable numbers of $Pax7^{+}$ myogenic precursor cells with no alterations in proliferation or apoptosis. These data implicated a downstream defect in myoblast differentiation. To test for a differentiation defect, we assayed the abundance of $Myog^{+}$ cells (Fig. 9P, Q) and found a significant increase in the percentage of $Myog^{+}$ cells within the EDL muscle of *Smyd1* CKO embryos (Fig. 9R). These data indicate that Smyd1 affects late stage myoblast differentiation.

Fig. 9

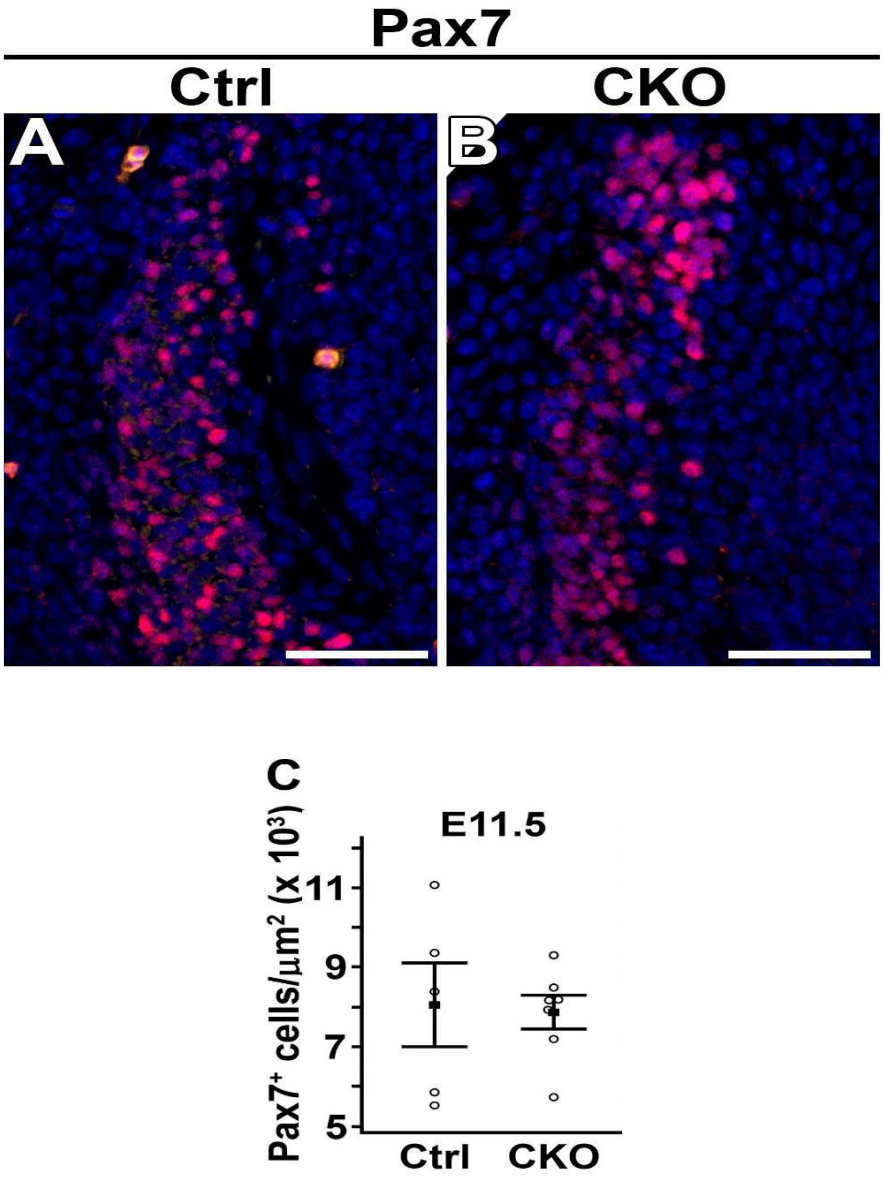

Fig. 9 Comparison of the number of Pax7^{+} myoblasts (muscle precursor cells) in the myotome at E11.5. Representative images of Pax7 immunofluorescence (red) [Fig. 9A-B]. Blue, nuclei (DAPI). No difference was observed in the number of Pax7^{+} cells normalized to cross-sectional area of the myotome (*n* ≥ 5 embryos/group) [Fig. 9C]. Scale bar = 50 um [Fig. 9A-B]. Ctrl, control; CKO, conditional knockout.

Fig. 9 (Continued)

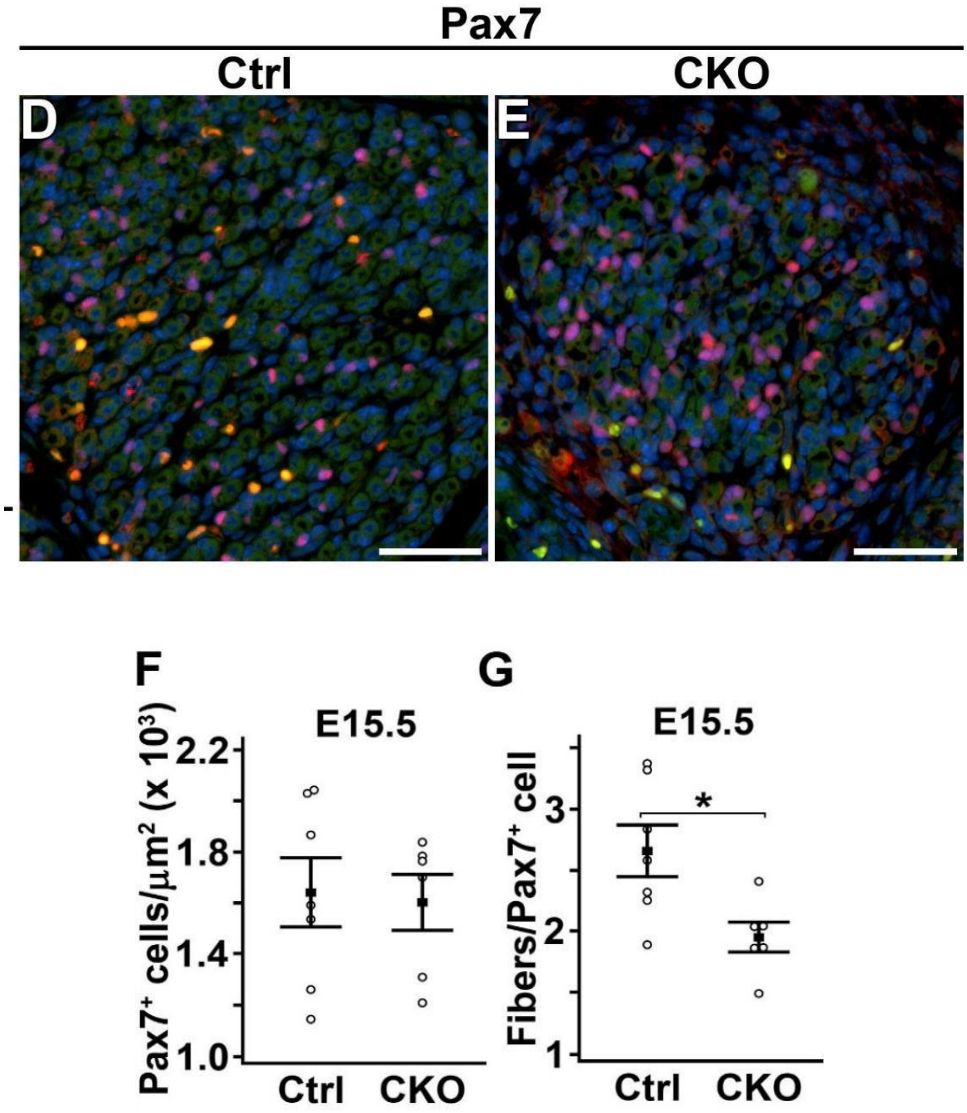

Fig. 9 (Continued) Comparison of the number of Pax7$^+$ myoblasts in the EDL muscle at E15.5. Representative images of Pax7 immunofluorescence (red). Green, myofibers (auto fluorescence) and Blue, nuclei (DAPI) [Fig. 9D-E]. No difference was observed in the number of Pax7$^+$ cells normalized to cross-sectional area of the EDL [Fig. 9F]; however, *Smyd1* CKO muscle exhibited less myofibers per Pax7$^+$ cell [Fig. 9G] ($n \geq 6$ embryos/group). *P < 0.05, **P < 0.01, Student's *t* test. Error bars indicate SEM. Scale bar = 50 um [Fig. 9D-E]. Ctrl, control; CKO, conditional knockout.

Fig. 9 (Continued)

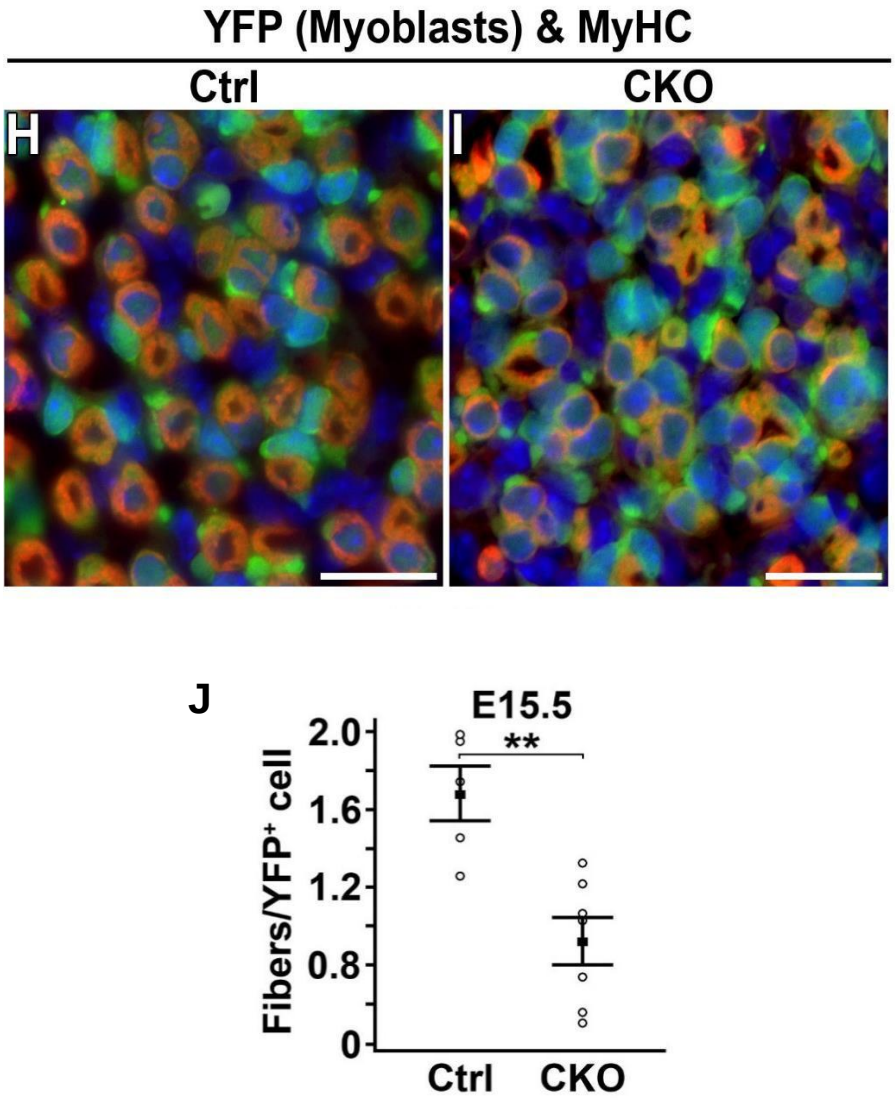

Fig. 9 (Continued) Comparison of the number of fibers relative to myoblasts in the EDL muscle at E15.5. Myoblasts were identified as non-myofiber YFP^+ cells. YFP expression is the result of recombination of the *Rosa26*^{YFP} allele by *Myf5*^{cre} and represents the *Myf5* lineage. Representative images of immunofluorescence for YFP (green) and MyHC (red) [Fig. 9H-I]. *Smyd1* CKO muscle exhibited less myofibers per myoblast [Fig. 9J] ($n \geq 5$ embryos/group). *$P < 0.05$, **$P < 0.01$, Student's *t* test. Error bars indicate SEM. Scale bars = 20 μm [Fig. 9H-I]. Ctrl, control; CKO, conditional knockout. YFP, yellow fluorescent protein; MyHC, myosin heavy chain.

Fig. 9 (Continued)

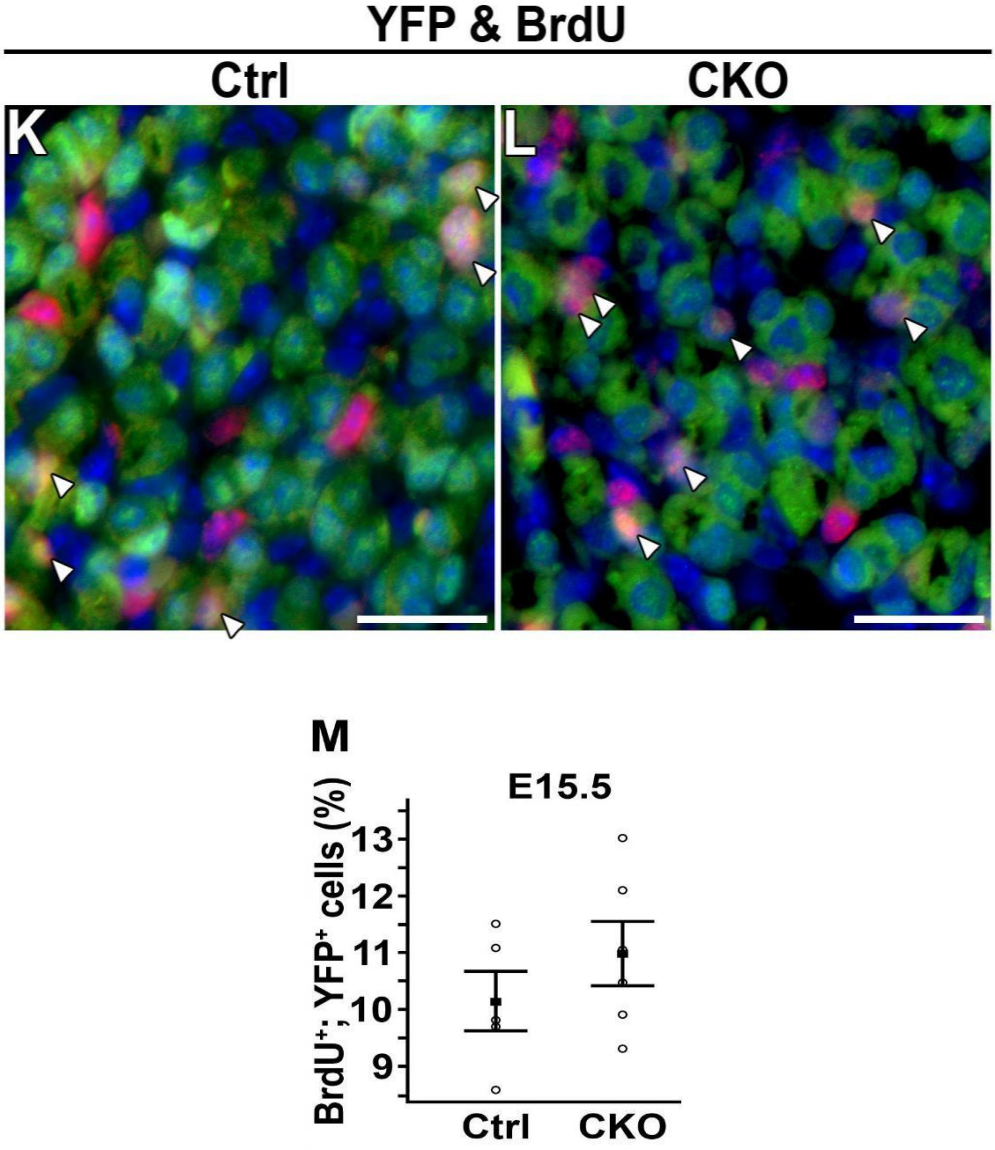

Fig. 9 (Continued) Comparison of myoblast proliferation within the EDL at E15.5. BrdU was administered 4 hours prior to sacrifice. Representative images of YFP (green) and BrdU (red) immunofluorescence [Fig. 9K-M]. No difference was observed in the percentage of $BrdU^+$ myoblasts (double positive cells) [Fig. 9M] ($n \geq 5$ embryos/group). *P < 0.05, **P < 0.01, Student's *t* test. Error bars indicate SEM. Scale bars = 20 μm [Fig. 9K-L]. Ctrl, control; CKO, conditional knockout. BrdU, bromodeoxyuridine.

Fig. 9 (Continued)

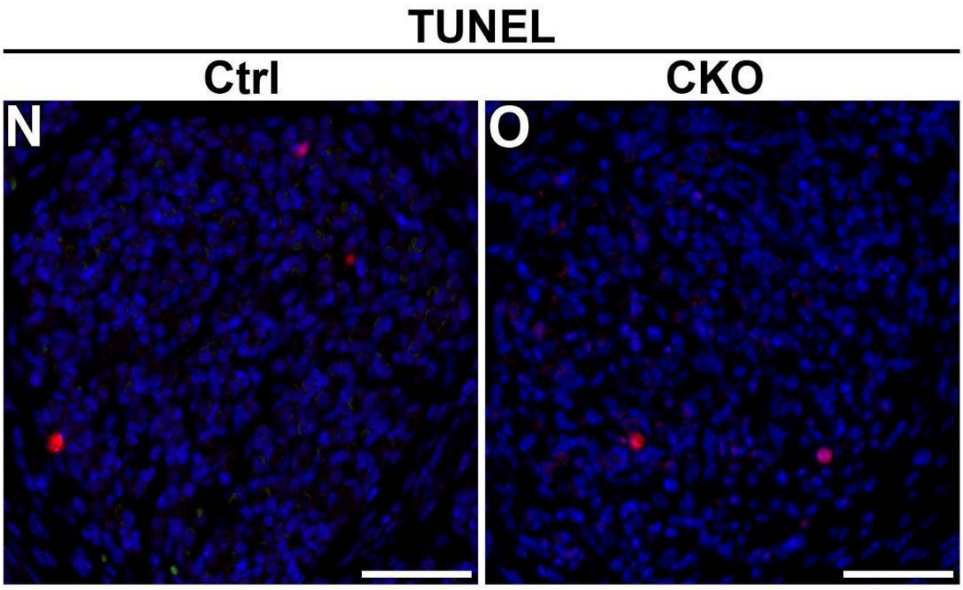

Fig. 9 (Continued) Comparison of apoptosis within the EDL at E15.5 by TUNEL assay. No difference was observed. Very few (1-2) TUNEL positive cells (red) were observed per EDL cross-section in both controls and CKOs (*n* ≥ 5 embryos/group) [Fig. 9N-O]. Blue, nuclei (DAPI). Scale bar =50 um. Ctrl, control; CKO, conditional knockout. TUNEL, terminal deoxynucleotidyl transferase dUTP nick end labeling.

Fig. 9 (Continued)

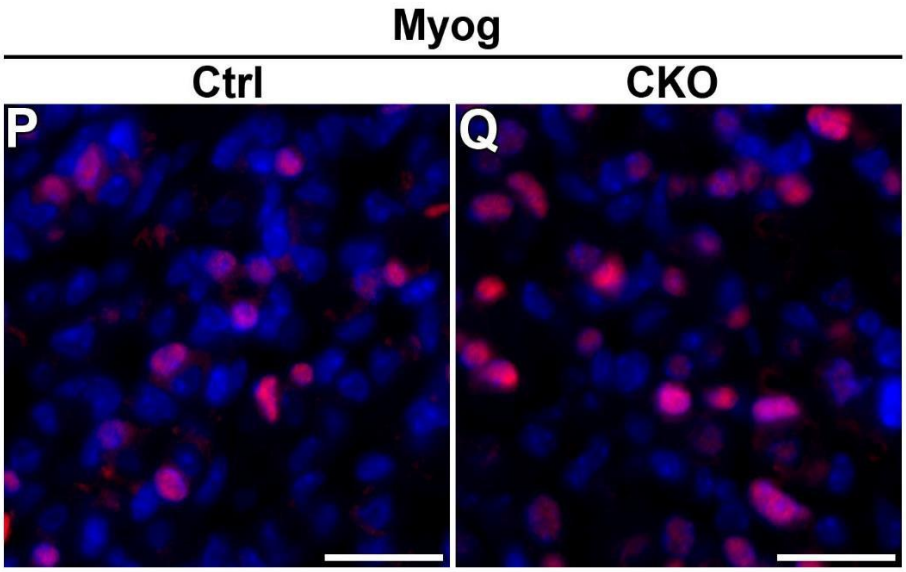

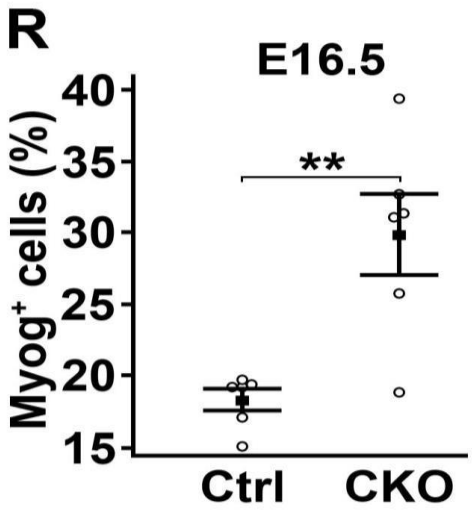

Fig. 9 (Continued) Comparison of the number of Myog$^+$ cells in the EDL at E16.5. Representative images of Myog immunofluorescence (red) [Fig. 9P-Q]. *Smyd1* CKO exhibited a higher percentage of Myog$^+$ cells than controls [Fig. 9R] (*n* = 6 embryos/group) Blue, nuclei (DAPI). *P < 0.05, **P < 0.01, Student's *t* test. Error bars indicate SEM. Scale bars = 20 μm [Fig. 9P-Q]. Ctrl, control; CKO, conditional knockout.

Smyd1 CKO embryos exhibit perinatal lethality.

Embryos from the cross *Myf5$^{cre/+}$; Smyd1$^{+/-}$* x *Smyd1$^{flox/flox}$; Rosa26$^{YFP/YFP}$* were recovered at various developmental stages (Table 3). The expected Mendelian percentage (25%) of CKO embryos were observed at all stages of gestation. However, embryos recovered at E17.5 or E18.5 were motionless. Less than the expected number of *Smyd1* CKO pups were found on the day of birth (postnatal day 0) and those that were identified were dead.

Smyd1 is predominantly expressed only in cardiac and skeletal muscle. Conditional deletion of Smyd1 in the heart was previously shown to cause embryonic lethality in mice. One of the possibilities causing perinatal lethality of Smyd1 CKO embryos could be leakiness of Myf5*cre* in cardiac tissue leading to improper heart development. In order to rule out this possibility, heart sections from control and Smyd1 CKO embryos at E18.5 were stained with Hematoxylin and Eosin, to assess overall tissue morphology. Hearts from both the groups looked normal and no obvious cardiac malformations could be detected in Smyd1 CKO embryos (Fig. 10A). Immuno-fluorescence for GFP using heart sections from control and Smyd1 CKO embryos at E15.5 revealed a random, non-specific pattern of few cells that stained positive for GFP expression and hence also for the expression of Cre (Fig. 10B). It remains to be determined whether the GFP positive cells in the hearts are fibroblasts or cardio-myoblasts. Since our control embryos also carry a few, random GFP positive cells in the

heart, loss of Smyd1 by Myf5-cre activation in GFP positive cells is unlikely to cause perinatal lethality observed in Smyd1-myf5cre-CKOs. *Smyd1* deletion in the myogenic lineage produces perinatal lethality likely due to inability to breathe right after birth.

Table 3 Smyd1 CKO embryos exhibit perinatal lethality

Stage	**Embryos Recovered**	**Expected**	**Observed**
E9.5	20	5	7
E10.5	196	49	49
E11.5	9	2.25	2
E13.5	48	12	10
E14.5	8	2	1
E15.5	142	35.5	30
E16.5	19	4.75	5
E17.5	31	7.75	4 (motionless)
E18.5	16	4	4 (motionless)
P0	53	13.25	6 (dead)

E, embryonic day; P, postnatal day

Fig. 10A

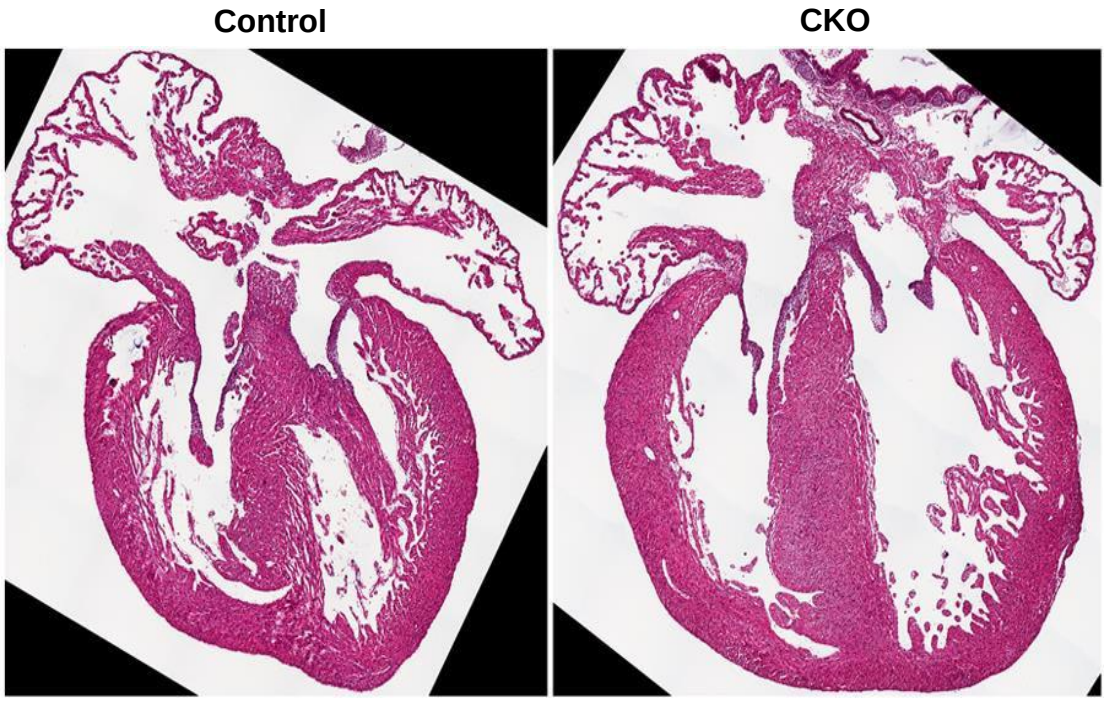

Fig. 10A H&E staining of E18.5 embryonic hearts shows no obvious cardiac malformation in Smyd1 CKOs. CKO, conditional knockout.

Fig. 10 (Continued)

Control **CKO**

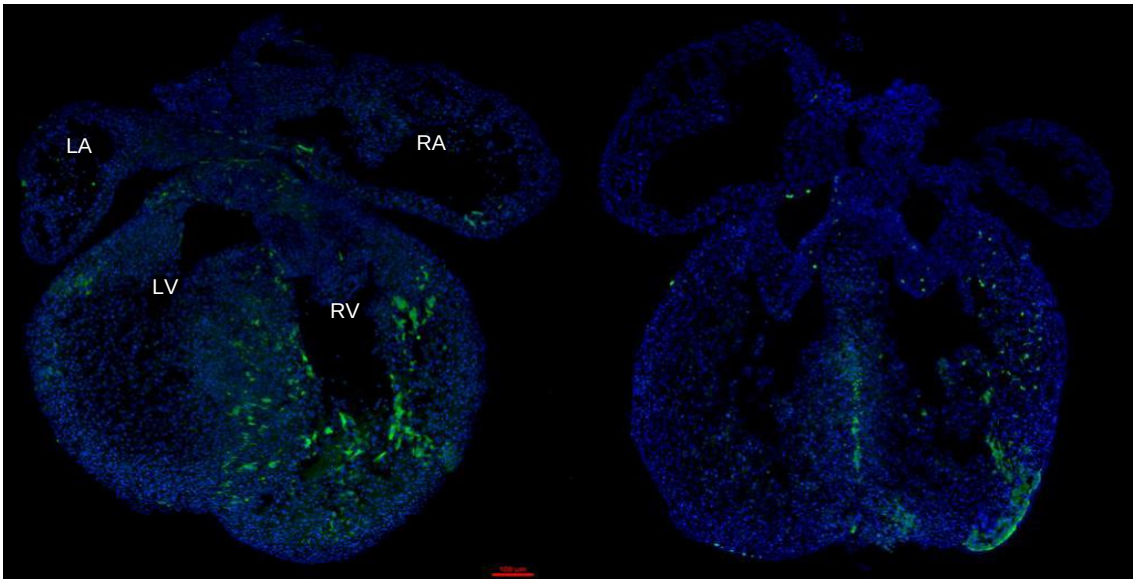

Fig. 10B (Continued) Immuno-staining embryonic hearts at E15.5 for GFP (green) reveals a random pattern of Myf5 expressing cells in both control and CKO embryos [Fig. 10 B]. Blue, nuclei (DAPI). CKO, conditional knockout.

Smyd1 knockdown in C2C12 myoblasts impairs fusion and blocks myotube hypertrophy. We employed the C2C12 mouse myoblast cell line to determine if *Smyd1* knockdown affects myoblast fusion or myotube growth. Previous studies reported that expression of *Smyd1* increases during myoblast differentiation (Li et al., 2009; Sims et al., 2002). First, we confirmed these reports by comparing Smyd1 protein levels in undifferentiated myoblasts vs. differentiated myotubes. Smyd1 protein was below the detectable threshold in undifferentiated myoblasts, but steadily increased after 1 to 5 days in differentiation medium (Fig. 11A). To reduce Smyd1 levels, C2C12 myoblasts were infected with lentivirus expressing shRNA against *Smyd1* or a non-specific control shRNA. After five days in differentiation medium, Smyd1 protein levels were reduced in two independently derived C2C12 clones that received *Smyd1* shRNA (1.5-fold and 3.1-fold, respectively). The clone that received the control lentivirus expressed Smyd1 at a similar level to that of the parental cell line (Fig. 11B). These clones were allowed to undergo differentiation for five days and then immuno-stained with a pan-MyHC antibody. *Smyd1* knockdown resulted in thin, hypotrophic myotubes (Fig. 11C, D). Myotube hypertrophy, as quantified by measuring myotube width at widest point on the myotube (*n* = 35-60 myotubes/group x three technical replicates), was significantly decreased in cells that received *sh*RNA against *Smyd1* (Fig. 11F). As revealed by the distribution of myotubes plotted according to their width (Fig. 11G), *Smyd1* knockdown cell lines showed an increased number of small diameter myotubes. Next, a myoblast fusion index was

calculated by dividing the number of nuclei incorporated into myotubes by the total nuclei in each field of view. *Smyd1* knockdown resulted in significantly fewer nuclei integrated into myotubes (Fig. 11E). These data indicate that Smyd1 regulates both myoblast fusion and myotube hypertrophy and support our *in vivo* observation of impaired myoblast differentiation in the *Smyd1* CKO.

Fig. 11

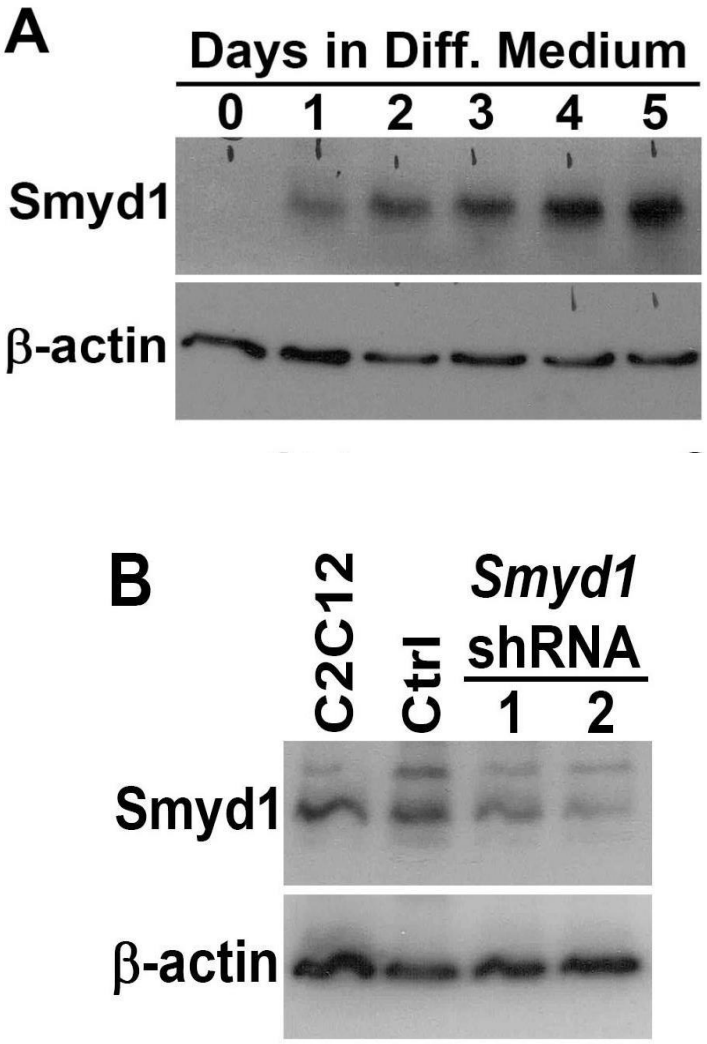

Fig. 11 Western blots - Smyd1 protein expression increased throughout the course of myoblast differentiation [Fig. 11A]. Smyd1 protein levels were reduced in cell lines stably expressing shRNA against Smyd1 [Fig. 11B]. The C2C12 lane contains extract from the parental cell line. The Ctrl lane contains extract from a cell line stably expressing non-specific control shRNA. Diff., differentiation.

Fig. 11 (Continued)

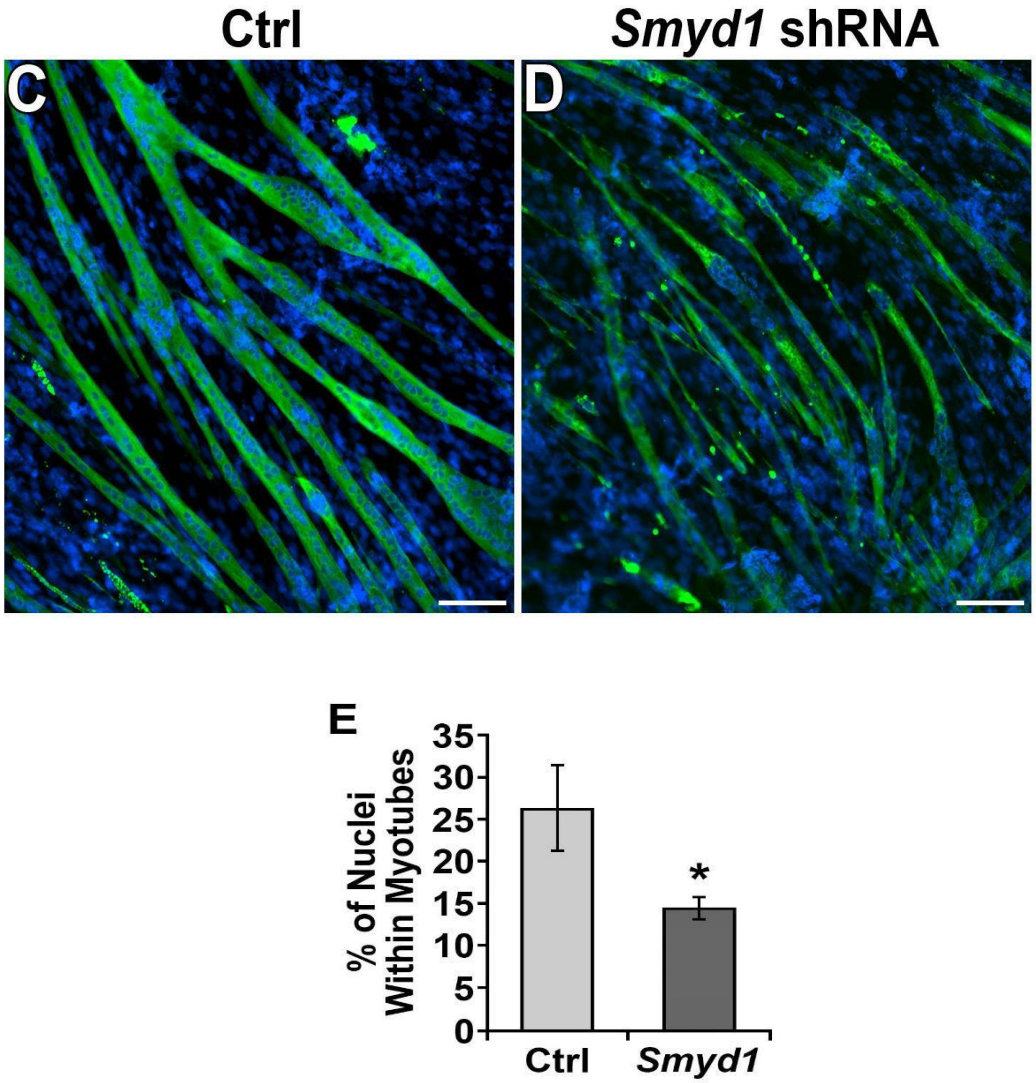

Fig. 11 (Continued) Knockdown of *Smyd1* led to thinner myotubes. Representative images of C2C12 cells expressing control shRNA [Fig. 11C] or *Smyd1* shRNA [Fig. 11D] after 5 days in differentiation medium. Myotubes were identified by immunofluorescence for myosin (green). Blue, nuclei (DAPI). *Smyd1* knockdown impaired myoblast fusion [Fig. 11E]. Myoblast fusion index was calculated by dividing the number of nuclei within myotubes by the total number of nuclei (*n* = 9 replicates/group). Scale bar = 100 um.

Fig. 11 (Continued)

F

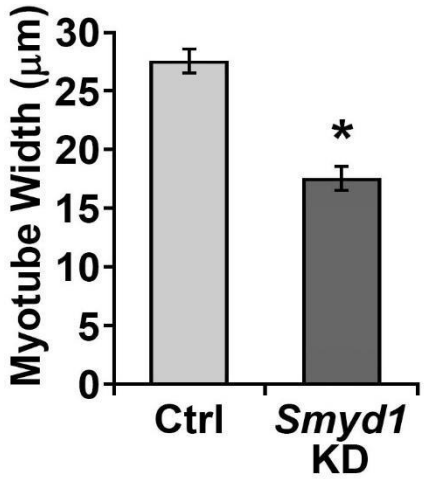

G

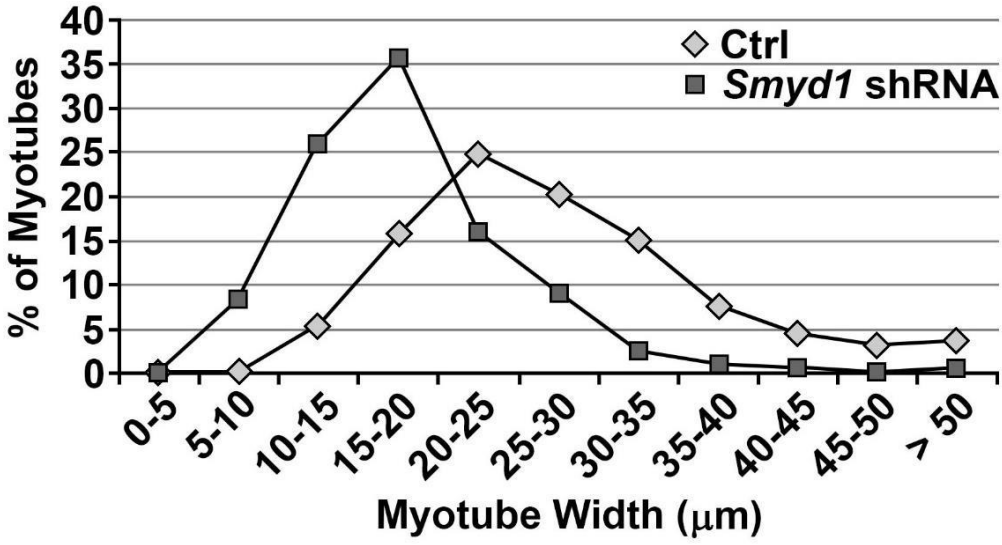

Fig. 11 (Continued) Smyd1 knockdown impaired myotube hypertrophy. Down-regulation of Smyd1 led to significant down-regulation in mean myotube width [Fig. 11F] and distribution of myotube widths [Fig. 11G] (n = 18 replicates/group). *P < 0.05, Student's t test. Error bars indicate SEM. Ctrl, control; Diff., differentiation.

Conditional knock-out of Smyd1 in myocytes preferentially affects only fast twitch muscle fibers

Smyd1 was also deleted in differentiated muscle cells (myocytes) using *Myf6-cre* (Fig. 12). This conditional deletion of Smyd1 at a later developmental stage, allowed for a dissection of its role in proliferating myoblasts versus differentiated myocytes. Unlike Smyd1-myf5cre-CKOs, skeletal myocyte specific deletion of Smyd1 is not embryonic lethal. Smyd1-myf6cre-CKOs are viable and exhibit characteristic features of Centro-nuclear myopathy (data not shown).

Interestingly Smyd1 loss only appears to affect fast-twitch muscle fibers. Western blots from extracts of tibialis anterior muscle, which is predominantly composed of fast-twitch muscle fibers, of six-week-old mice show upregulation of myosin heavy chain protein in Smyd1-myf6cre-CKOs (Fig. 13A). Increase in Akt protein levels, which has been previously shown to cause skeletal muscle hypertrophy is also observed, along with a mild increase in its downstream effector S6 kinase (Fig. 13A), in Smyd1-myf6cre-CKOs. However, levels of Akt and S6 kinase appeared unchanged in extracts of quadriceps muscle (Fig. 13B), which consists of an equal mix of fast and slow twitch muscle fibers. Similarly, extracts from soleus muscle, which consist mostly of slow twitch muscle fibers, showed similar level of pan myosin expression (Fig. 13C) between six-week-old control and Smyd1-myf6cre-CKOs.

Thus, although Smyd1 is expressed at equivalent levels in both slow and fast-twitch muscle types and is deleted from all muscle groups examined in Smyd1-myf6cre-CKOs, Smyd1 loss mainly seems to have affected only fast-twitch muscle fibers. This finding is in agreement with studies done in zebra fish (Just et al., 2011). Interestingly, while Smyd1 is expressed at low levels in proliferating myoblasts as compared to differentiated myofibers (Fig. 11A), Smyd1 deletion at the former stage is lethal.

Fig. 12

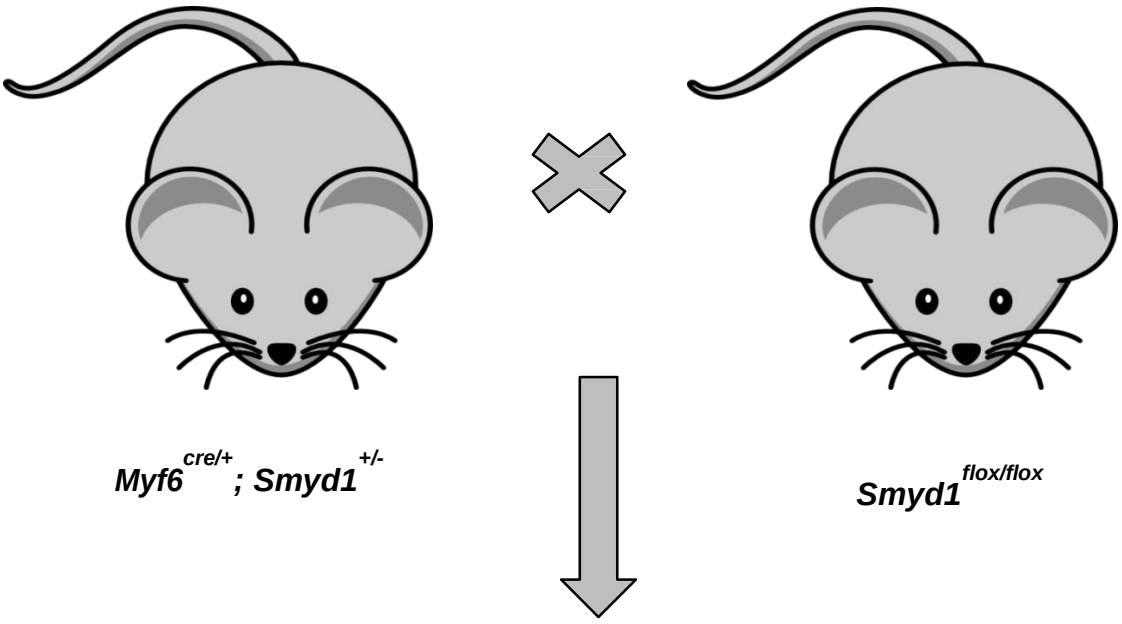

Fig. 12 Mating scheme to show mouse bred to delete Smyd1 in differentiated myocytes

Fig. 13

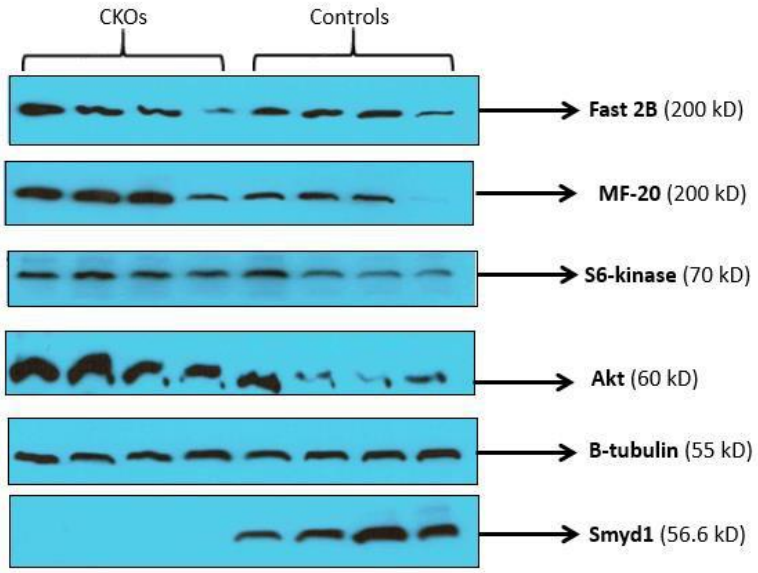

Fig. 13A Western blots with extracts from Tibialis anterior muscle (TA), which mostly consists of fast twitch muscle fibers, from 6 week old control and Smyd1-myf6cre-CKO mice show up-regulation of Akt signaling and myosin production in the knock-outs. CKO, conditional knockout.

Fig. 13 (Continued)

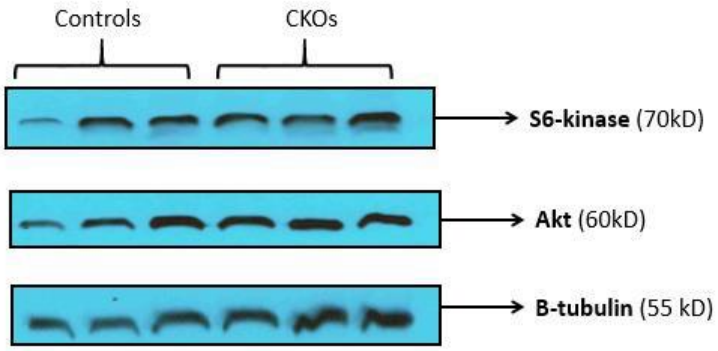

Fig. 13B (Continued) Western blots with extracts from quadriceps muscle, which consists of an equal mix of fast and slow twitch muscle fibers of 6 week old control and Smyd1-myf6cre-CKO mice indicate Akt signaling remains unchanged in the CKOs. CKO, conditional knockout.

Fig. 13 (Continued)

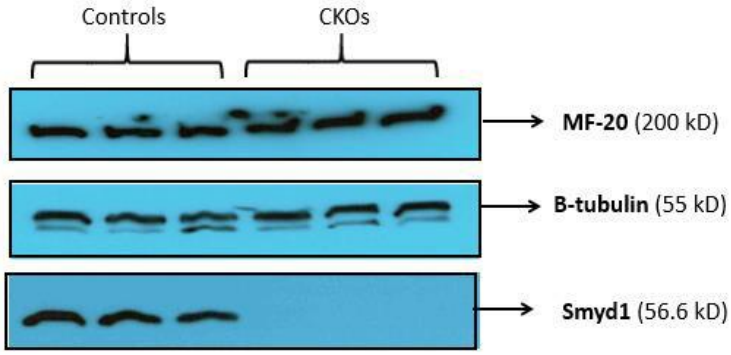

Fig. 13C Western blots with extracts from soleus muscle, which mostly consists of slow twitch muscle fibers, from 6 week old control and Smyd1-myf6cre-CKO mice indicate no change in myosin production. CKO, conditional knockout.

Cytoskeletal proteins identified in the Smyd1 immuno-precipitation complex through mass spectrometric analysis

Immuno-precipitation (IP) with antibody specific for Smyd1 was carried out using quadriceps muscle extracts of mice in order to identify proteins interacting with Smyd1. Extracts from Smyd1-myf6cre-CKO mice served as negative control. Smyd1 was detected in the IP complex from wild type mice through western blot (Fig. 14A), hence proving it's successful immuno-precipitation. All the protein fragments identified through mass spectrometric analysis in the wild type sample have been documented in Table 4.

One of the peptide fragments detected was for Myosin heavy chain 2 (Myh2), which supports previous studies performed in zebrafish where Smyd1 was found to physically interact with myosin (Just et al., 2011). Peptide fragments of Actc1 were identified in IP complex from both wild type and Smyd1 CKO mice and hence can be ruled out as false positive hits. Cytoskeletal proteins identified in Smyd1 IP fit well with the observation that most of the Smyd1 in differentiated muscle fibers resides in the cytoplasm.

Fig. 14

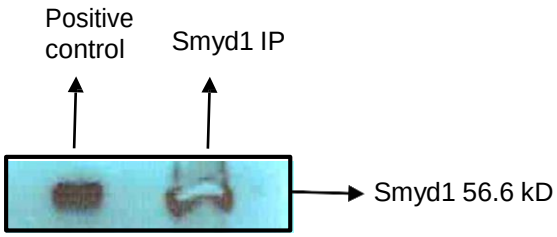

Fig. 14 Successful immuno-precipitation (IP) of Smyd1 from quadriceps muscle extracts of six week old control mice as detected through western blotting

Table 4 Proteins identified in the immuno-precipitation complex of Smyd1 through MALDI-TOF

Protein identified	Precursor mass in Daltons (Da)	False positive rate (FPR) in %	Peptide fragment detected	Comments
Smyd1	2834.360	0.0004	EAALNNQPMQ VMAEPSNEPA PALFHK	SET and MYND domain containing protein 1. Striated muscle specific histone lysine methyl transferase
Desmin	1557.848, 1768.755	0.34, 0.000019	FASEANGYQD NIAR, DGEVVSEATQ QQHEVL	Intermediate filament protein
Vimentin	1533.797, 1254.519	0.23, 0.01	KVESLQEEIA FLK, LGDLYEEEMR	Intermediate filament protein
Tpm3	1243.658	0.51	IQLVEEELDR	Tropomyosin 3 Provides stability to actin filaments and regulates access of other actin binding proteins
Myh2	1855.853	0.05	SSDAEMAVFGEAAPYLR	Myosin heavy chain 2. Functions in skeletal muscle contraction

(Table 4 continued) Protein identified	Precursor mass in Daltons (Da)	False positive rate (FPR) in %	Peptide fragment detected	Comments
Zfp82	1492.706	8.4	VTMGDPGRTN SETK	Tumor suppressor that inhibits cell proliferation by inducing apoptosis
Actc1	1790.892, 1515.749, 3196.6096	0.000015 0.63, 0.31	SYELPDGQVI TIGNER, IWHHTFYNEL R, TTGIVLDSGD GVTHNVPIYE GYALPHAIMR	Actin, alpha, cardiac muscle1. **False positive hit**. Also detected in negative control IP experiment from Smyd1-myf6cre-CKO muscle
Krt71	1475.7853	5.7	FLEQQNQVLQ TK	Keratin - Intermediate filament protein. Most common form of contamination in mass spec. data
Krt78	1383.690	0.06	SLNNQFASFI DK	Keratin - contamination
Trypsin	2283.180	2.1	IITHPNFNGN TLDNDIMLIK	Result of autolysis of trypsin enzyme used for fragmentation of immuno-precipitation complex

Chapter IV

Discussion

DISCUSSION

Spatial and temporal expression of Smyd1 during myogenesis. Previous reports of Smyd1's subcellular localization during myoblast differentiation have been limited to endogenous Smyd1 in C2C12 cells and transgenic expression of Myc-tagged Smyd1 in zebrafish. In C2C12 cells, Smyd1 shuttles from the nucleus to the cytoplasm during myoblast differentiation (Berkholz et al., 2014; Sims et al., 2002). Zebrafish expressing Myc-Smyd1 show primarily cytosolic localization in both myoblasts and myotubes (Li et al., 2011). For C2C12 cells, we found Smyd1 to be both nuclear and cytoplasmic in myoblasts, but primarily cytoplasmic in myotubes. Importantly, we found that *in vivo*, as with C2C12 cells, Smyd1 protein localized to both the nucleus and cytoplasm of $Myog^{+}$ myoblasts within the myotome. Little to no Smyd1 was detectable in $Pax7^{+}$ myogenic progenitor cells and $Myog^{+}$ cells could be found with or without Smyd1 expression. These observations indicate that Smyd1 is downstream of Myog, becoming expressed in differentiating myoblasts. Importantly, this is the myogenic stage affected by the absence of Smyd1. *Smyd1* CKO embryos exhibited increased $Myog^{+}$ myoblasts and fewer myofibers. In differentiated muscle fibers, Smyd1 primarily localized to the sarcoplasm. Within the sarcoplasm, Smyd1 localized within bands opposite/non-overlapping to that of α-actinin, consistent with previous reports of Smyd1's localization to the sarcomeric M-line in zebrafish fast-twitch muscles (Just et al., 2011; Li et al., 2011).

Not only does Smyd1's subcellular localization change during myoblast differentiation, but protein levels also greatly increase and most (if not all) of the extra protein ends up in the sarcoplasm. The large increase in Smyd1 protein expression during differentiation is most apparent in western blots, where levels are almost undetectable in undifferentiated C2C12 myoblasts and extremely abundant after a few days in differentiation medium (Fig. 11A). This is also supported by immunofluorescence experiments because exposure times to detect Smyd1 in myotubes/fibers are much shorter than for myoblasts (Fig. 5P vs. Fig. 5F, K). Furthermore, when differentiated C2C12 cells are stained for Smyd1, the undifferentiated myoblasts in the culture appear negative because of the high abundance in the myotubes (Fig. 5D). Nuclear Smyd1 is barely detectable in myotubes/fibers *in vivo* or *in vitro*; however there appears to be low nuclear levels that are difficult to detect due to the high abundance in the sarcoplasm. Collectively, these observations support the idea that Smyd1 is both an epigenetic modulator of transcription as well as a sarcoplasmic regulator of myofibrillogenesis.

Defective second wave myogenesis. No gross abnormalities, changes in gene expression or abundance of $Pax7^{+}$ myoblasts were detected in *Smyd1* CKO embryos at E11.5 (Fig. 6 and Fig. 9A-C) Hence, *Smyd1* deletion did not appear to affect the first wave of myogenesis, which occurs from E10.5 to E12.5 in mice

(Biressi et al., 2007b). However, we found reduced numbers of myofibers as well as altered gene expression for a number of skeletal muscle specific genes during the second myogenic wave, which occurs from E14.5 to E17.5 (Biressi et al., 2007b). *Smyd1* CKO embryos exhibited a greater loss of secondary than primary myofibers during the second myogenic wave. This may be due to unique functions for Smyd1 in fast-twitch fibers. Based on contractile protein expression, previous literature suggests that primary myofibers are similar to adult slow-twitch fibers and secondary fibers are more akin to adult fast-twitch fibers (Biressi et al., 2007b). *Smyd1* mutant zebrafish exhibit defective myofibrillogenesis specifically in fast-twitch fibers (Just et al., 2011). Likewise, CKO of *Smyd1* in differentiated myofibers (perinatal CKO post-myogenesis) results in centronuclear myopathy specifically in fast-twitch muscles (Stewart et al. manuscript in review). Our observation that loss of *Smyd1* more greatly disrupted formation of secondary fibers supports the idea that *Smyd1* may be more important for the stability and/or function of fast-twitch fibers. These data suggest that although *Smyd1* is expressed in all fiber types in mammals, it may perform selective functions in different fiber types. Smyd1's fast-twitch fiber-specific functions may be more critical for the growth and survival of myofibers during myogenesis.

We also noticed partial penetrance of the phenotype in *Smyd1* CKO embryos in terms of reduction in primary and secondary muscle fibers during the second myogenic wave. A few CKOs had a very severe loss of muscle fibers; most CKOs had a modest but noticeable reduction. Such variability might be due to slight differences in the timing of *Smyd1* deletion or variability in the percentage of myoblasts harboring a total loss of *Smyd1*. The mice used for this study were of a mixed B6;129 genetic background, which could conceivably contribute to this variability.

Our evidence suggests Smyd1 is important for late-stage myoblast differentiation. Both control and *Smyd1* CKO muscles exhibited similar abundance of $Pax7^{+}$ myogenic progenitor cells, rates of proliferation and apoptosis in the EDL at E15.5, the midpoint of the second myogenic wave. We found no evidence for degeneration as *Smyd1* CKOs did not exhibit TUNEL positive myofibers, alterations in atrophy gene expression or reduction in myofiber diameter. What we did find was fewer myofibers relative to myoblasts and increased numbers of $Myog^{+}$ myoblasts. These data suggest impaired myoblast differentiation and are consistent with the impaired myoblast fusion observed in *Smyd1* knockdown C2C12 cells (Fig. 15).

The stage in mouse embryogenesis when motor neurons first make contact with developing muscle fibers is also during the second myogenic wave (Rossi and Messina, 2014). Interaction between newly forming muscle fibers and neurons is necessary for further development of myofibers. Failure of motor neurons to properly interact with developing myofibers leads to dis-integration of both primary and secondary muscle fibers, with the latter being more severely affected (Biressi et al., 2007a). This phenotype is very similar to what we observe in our *Smyd1* CKO mouse embryos. Hence it is possible that Smyd1 plays a role in relaying a survival cue from newly formed neuromuscular junctions. However, data from C2C12 cells argues against this being the primary defect. Knock-down of *Smyd1* expression in C2C12 cells led to hypotrophic, poorly differentiated myotubes with reduced fusion index and impaired myofiber growth. These *in vitro* data do not support the idea that myofiber loss was due to negative effects on innervation, but rather due to intrinsic effects on myoblast differentiation or myofiber growth. It appears from immunofluorescence experiments that individual *Smyd1* CKO myofibers contain less total MyHC protein (CKO myofibers exhibit weaker anti-MyHC fluorescence intensity than control myofibers) (Fig. 8A-D). This observation implicates Smyd1 as a positive regulator of muscle gene expression underlying myofiber growth.

Smyd1 CKO embryos showed altered expression of three major myogenic transcription factors (*Pax3*, *Myf5* and *Myf6*) only during the second wave of myogenesis (Fig. 8R, N, O). Reduced *Myf5* expression, which is temporally downstream of *Pax7* during myogenesis, indicates that there may be a defect in myoblast differentiation or that Smyd1 regulates the myoblast differentiation gene expression program. Reduced expression of *Myf5* was not the result of the $Myf5^{cre}$ knock-in because our control embryos also expressed *cre* (Controls were $Myf5^{cre/+}$; $Smyd1^{flox/+}$). Increased expression of *Pax3* could be due to a compensatory feedback loop due to impaired myoblast differentiation. *Pax3* is more highly expressed in primary wave myoblasts and myofibers than in their secondary wave counterparts (Biressi et al., 2007b). Thus, increased *Pax3* expression opens the possibility that *Smyd1* CKO fetal myoblasts retain the gene expression signature of embryonic myoblasts, which may impair second wave myogenesis. Alternatively, increased *Pax3* could simply reflect the increased ratio of primary to secondary myofibers. *Myf6* is expressed late during myogenesis and it is the only MRF expressed in mature myofibers (Rhodes and Konieczny, 1989). Reduced *Myf6* expression would impair myofiber development, as seen in the *Smyd1* CKO; however, decreased *Myf6* mRNA could be a consequence of less total myofibers.

In zebrafish embryos, *Smyd1* knockdown did not affect the mRNA levels of various myosin isoforms, but did affect their protein levels (Just et al., 2011). It was apparent from anti-MyHC immunofluorescence that *Smyd1* CKO myofibers have less total MyHC protein than controls (Fig. 8A-D). Thus, our data are consistent with those from zebrafish models, in that loss of *Smyd1* resulted in reduced MyHC protein; however, we also observed reduced gene expression for several MyHC isoforms (*Myh3*, *Myh7* and *Myh8*) and α-actin (*Acta1*) (Fig. 8H-K). These alterations in gene expression could be a consequence of fewer myofibers, but also support the idea that Smyd1 positively regulates contractile protein gene expression. The latter hypothesis is supported by a recent article indicating that Smyd1 is essential for activation of muscle genes in rhabdomyosarcoma (Coda et al., 2015).

Edema and embryonic lethality. *Smyd1* CKO embryos are motionless when recovered on E17.5 or E18.5 and consistently die perinatally (Table 1). A very similar phenotype, including dorsal subcutaneous edema and perinatal lethality, was observed when *Smyd1* was deleted using *Myog-cre*, (T.L. Rasmussen and H.O. Tucker, unpublished observations). These data indicate that muscle contraction becomes impaired over time - essentially a mild version of the phenotype reported for zebrafish *Smyd1* mutants or knock-downs where muscle contraction was completely absent from myofiber inception (Just et al., 2011).

Failed myofibrillogenesis in zebrafish is thought to result from improper myosin folding or assembly (Just et al., 2011).

Almost all *Smyd1* CKOs exhibited subcutaneous edema reminiscent of the "amorphous connective tissue" reported for the *Myf5/MyoD* double knock-out mouse (Rudnicki et al., 1993), which completely lacks skeletal muscle. Thus, subcutaneous edema could be the consequence of muscle loss. Edema could also be the consequence of impaired circulation or lymphatic drainage. This is puzzling as *Smyd1* expression is restricted to striated muscles and $CD8^+$ T lymphocytes (Gottlieb et al., 2002; Hwang and Gottlieb, 1997). $Myf5^+$ progenitors give rise to skeletal muscle, brown adipose, some rib cartilage, dorsal skin and connective tissues ((Haldar et al., 2008) and Fig. 7C, D). Thus, vessels along the dorsal aspect of the embryo could be impacted by $Myf5^{cre}$. But, even if $Myf5^{cre}$ catalyzed *Smyd1* deletion in other tissues, it is unlikely to have an effect because *Smyd1* is not expressed in those tissues. This suggests depletion of Smyd1 from the skeletal muscle lineage has a non-cell autonomous effect on the circulatory/lymphatic system. We looked for heart defects, but found no obvious morphological abnormalities by histological analysis and there was no pericardial edema (data not shown). Although the striated muscle-specific expression pattern is well-documented, *Smyd1* could be expressed in a non-muscle cell type that is also in the *Myf5* lineage and important for proper circulation (e.g. dorsal

smooth muscle or endothelial cells). The other members of the SMYD family (*Smyd2 - 5*) exhibit broad expression in many cell types. Thus, it is not unreasonable to hypothesize that *Smyd1* expression is broader than currently known.

Collectively, our results indicate that inception of the skeletal myogenesis program does not require Smyd1, but downstream events do. Elimination of Smyd1 impairs myofiber development and alters myogenic gene expression during the second wave of mammalian skeletal myogenesis. In zebrafish, *Smyd1* is only critical for sarcomerogenesis in fast-twitch myofibers (Just et al., 2011). In contrast, in mice, where both fast- and slow-twitch fibers are multi-nucleated and interspersed, Smyd1 appears to be necessary for proper development of both fiber types during embryogenesis. Based on our studies and the current literature, Smyd1 is multi-functional and vital for diverse aspects of muscle biology via epigenetic effects on gene expression and protein-protein interactions that facilitate myofibrillogenesis. A challenging future objective is to identify the promoter/enhancer regions targeted by Smyd1 histone methyltransferase action and to determine the accompanying epigenetic consequences *in vivo*.

Fig. 15 Model for Smyd1 function during myoblast differentiation

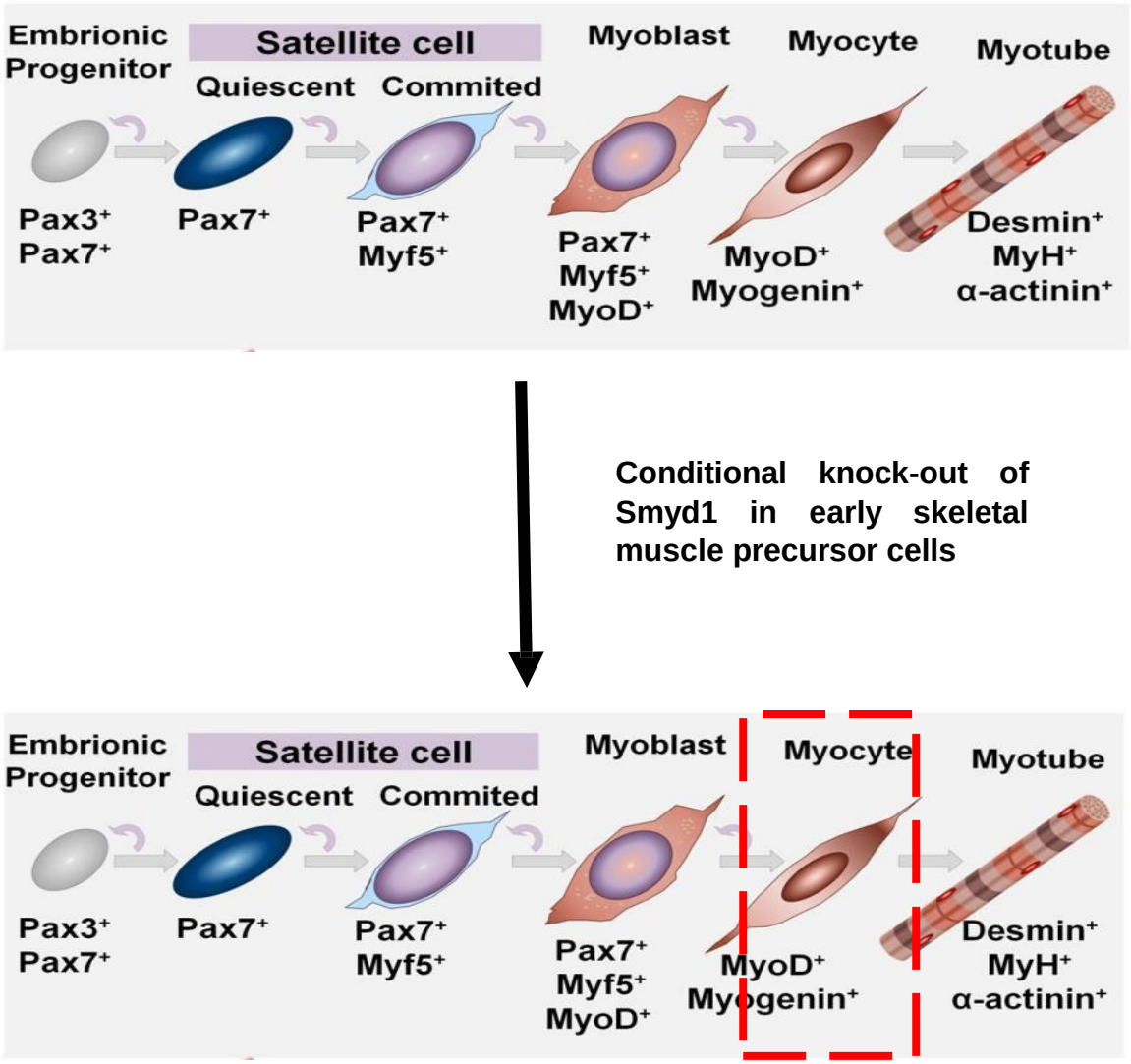

Fig. 15 Smyd1 deletion in skeletal muscle precursor cells led to their inefficient downstream differentiation. During skeletal myogenesis, MyoG expression declines upon fusion of myocytes into myotubes. Loss of Smyd1 resulted in a signficantly higher percentage of MyoG (Myogenin) positive cells in the conditional knock-out (CKO) embryos, implying an impairment in the ability of these myocytes to undergo downstream differentiation and fusion to form myotubes.

Chapter V
Materials and Methods

MATERIALS AND METHODS

Animals. *Smyd1$^{flox/flox}$* mice were developed in collaboration with Dr. Haley Tucker (University of Texas, Austin) (Rasmussen et al., 2015). *Smyd1$^{+/-}$* mice were generated by crossing *Smyd1$^{flox/flox}$* to the maternal deleter *Tg(Sox2-cre)* (Hayashi et al., 2003) (Jackson Laboratory, stock #8454). *Rosa26$^{YFP/YFP}$* and *Myf5$^{cre/+}$* mice were obtained from the Jackson Laboratory (stock #7903 and #10529, respectively). Mice for experimental analysis were obtained from the following cross: *Myf5$^{cre/+}$; Smyd1$^{+/-}$* x *Smyd1$^{flox/flox}$; Rosa26$^{YFP/YFP}$*. Controls were *Myf5$^{cre/+}$; Smyd1$^{flox/+}$; Rosa26$^{YFP/+}$*. CKOs were *Myf5$^{cre/+}$; Smyd1$^{flox/-}$; Rosa26$^{YFP/+}$*.

The following primers were used for genotyping: Cre-F: 5'-GCC ACC AGC CAG CTA TCA ACT C, Cre-R: 5'-TTG CCC CTG TTT CAC TAT CCA G, Smyd1-F: 5'-TCA TGA GAT GGG CAT GAG CC, Smyd1-R1 5'-GCA TAC GCA CAT GTG CTC GC, Smyd1-R2: 5'-CTC ACT TGC GTC CCA GTA CTT G. Smyd1-F/R1 identifies wild-type and flox alleles (432 bp and 552 bp, respectively). Smyd1-F/R2 identifies the null allele (~500 bp). Mice were euthanized by CO_2 inhalation followed by cervical dislocation. All experimental procedures involving mice were approved by the Institutional Animal Care and Use Committee of the University of Houston.

Tissue collection. Embryos were manually dissected in PBS immediately after euthanasia. For RNA or protein extraction, tissues were snap frozen in liquid nitrogen and stored at -80C. For H&E staining, tissues were fixed by overnight immersion in Bouin's fluid. For immunofluorescence, tissues were fixed overnight in 4% PFA in PBS and rinsed in 70% ethanol for ≥ 25 h prior to tissue processing. All tissues were dehydrated through a standard ethanol gradient, cleared in Histoclear (National Diagnostics, cat# HS-200) and embedded in Paraplast Plus® Tissue Embedding Medium (Statlab, cat# 2004). Seven to eight micron sections were prepared for histology.

Wholemount in situ hybridization. Wholemount *in situ* hybridization was performed following a standard protocol (Nagy, 2003). Digoxigenin (DIG)-labelled complementary RNA probes were prepared using a DIG RNA Labeling Kit (Roche, cat# 11 175 025 910). Hybridization and wash steps were automated using an InsituPro robot (Intavis AG). Hybridized probes were visualized by a color reaction using alkaline phosphatase-conjugated anti-DIG Fab fragments (Roche, cat# 11 093 274 910) and nitroblue tetrazolium and bromochloroindolyl phosphate (NBT-BCIP) reagents (Roche, cat# 11 681 451 001). Embryos were post-fixed in 4% paraformaldehyde-PBS and imaged in PBS. Probe sequence information is available upon request.

Western blotting. Western blot assays were carried out with either whole cell extracts obtained using RIPA buffer from C2C12 cells or frozen E16.5 embryos with head and internal organs removed, were homogenized in T-PER buffer (Life Technologies) according to the manufacturer's instructions along with protease and phosphatase inhibitors. The suspension was then centrifuged at 10,000 x g for 5 min. 50 µg of supernatant protein was solubilized in Laemmli Buffer and separated by 4-20% SDS-PAGE (Mini Protean II System, Bio-Rad Laboratories, Hercules, CA). The proteins were transferred onto 0.2 µm nitrocellulose membranes (Bio-Rad Laboratories). Membranes were blocked with 5% non-fat milk-TBST for 1 h at room temperature. Primary antibody recognizing Smyd1 (Santa Cruz, cat# sc-79080), myosin heavy chain (MyHC) (Developmental Studies Hybridoma Bank, clone MF-20) or β-actin-HRP (Santa Cruz I-19, cat# sc-1616) was diluted in 2.5% non-fat milk-TBST. Following overnight incubation at 4C with primary antibody, membranes were washed with TBST and then incubated with appropriate horseradish peroxidase-conjugated secondary antibody for 3 h at room temperature. Membranes were washed again, and visualized by chemiluminescence using SuperSignal West Pico Chemiluminescent Substrate (Thermo Scientific, Rockford, IL).

Histological analyses. H&E staining was performed using the standard protocol. Immunofluorescence was performed on 8 µm paraffin sections by using

1X casein for blocking. 10% normal serum-1X PBST as the antibody diluent (10x casein stock solution and normal serum were from Vector Labs). Primary antibodies were incubated overnight at 4C. Secondary antibodies were incubated for 1 h at room temperature. All slides were counterstained with DAPI and coverslips mounted with vecta-shield hard Set mounting medium (Vector Labs). Primary antibodies used were as follows: Smyd1 (Santa Cruz, cat# sc-79080), myosin heavy chain (Developmental Studies Hybridoma Bank, clone MF-20), α-actinin (clone EA-53, Sigma-Aldrich, cat# A7811), GFP (Abcam, cat# ab6662) and Pax7 (Developmental Studies Hybridoma Bank).

To assay cell proliferation, pregnant mice were weighed and injected with 10ml/kg BrdU Labeling Reagent (Invitrogen, catalog# 00-0103) 4 hours before sacrifice. Immunofluorescence was performed as described above with anti-BrdU monoclonal antibodies (Developmental Studies Hybridoma Bank, clone G3G4). Apoptosis was assayed using the Click-iT® Plus TUNEL Assay kit (Life technologies, Catalog#C10618) according to the manufacturer's instructions.

Microscopy. Stereoimages (bright field and fluorescence) were captured with Leica MZ10F stereomicroscope and the extended depth of focus feature of LAS v3.7 software (Leica Microsystems, Wetzlar, Germany). Brightfield and epifluorescence images of tissues sections were obtained using a Nikon Ti-E inverted microscope equipped with a DS-Fi1 5-megapixel color camera (Nikon

Instruments), a CoolSNAP HQ2 14-bit monochrome camera (Photometrics, Tucson, AZ) and NIS Elements software v4.13 (Nikon Instruments).

Real-time PCR. Total RNA was extracted from whole E11.5 embryos and E15.5 embryos with head and internal organs removed using TRIzol reagent according to the manufacturer's protocol (Life Technologies, Carlsbad, CA). mRNA levels were measured using TaqMan gene expression assays with 6-carboxyfluorescein (FAM)-labelled probes from Applied Biosystems (Life Technologies) (Mm01332463_m1 for *Myh3*, Mm01319006_g1 for *Myh7*, Mm01329494_m1 for *Myh8*, Mm01203489_g1 for *Myod1*, Mm00446195_g1 for *Myog*, Mm01354484_m1 for *Pax7*, Mm00468267_m1 for *Eno3*, Mm01321487_m1 for *Ckm*, Mm00808218_g1 for *Acta1*, Mm01185221_m1 for *Trim63*, Mm00499523_m1 for *Fbxo32*) and custom oligos for *Pax3* (Pax3-F: 5'-CCA GAG GGC GAA GCT TAC C, Pax3-R: 5'-GTT GAT TGG CTC CAG CTT GTT T, Pax3-Probe: 5'-TCT GGT TTA GCA ACC GCC GTG CA), *Myf5* (Myf5-F: 5'- AGC AGC TTT GAC AGC ATC TAC TGT, Myf5-R: 5'-AAT GCT GGA CAA GCA ATC CAA, Myf5-Probe: 5'-TGC TGC AGA TAA AAG CTC CGT GTC CA) and *Myf6* (Myf6-F: 5'- AGC TAC AAA CCC AAG CAA GAA ATT, Myf6-R: 5'-CCT GGA ATG ATC CGA AAC ACT T, Myf6-Probe: 5'-TGC GGA TTT CCT GCG CAC CTG) (Biosearch Technologies, Petaluma, CA). The level of *Gapdh* mRNA was used for normalization. The PCR was run using an ABI Prism 7900HT

thermocycler and SDS2.1 software (Applied Biosystems). Data were analyzed by the comparative ΔΔCT method.

Cell culture. The mouse skeletal myoblast cell line C2C12 was obtained from ATCC (cat# CRL-1772). C2C12 cells were routinely cultured in their undifferentiated state in high glucose DMEM supplemented with 20% fetal bovine serum and 1X antibiotic-antimycotic (Life Technologies, cat# 15240-096) at 37 ^{0}C and 5% CO_2. Differentiation was induced by switching the medium to high glucose DMEM supplemented with 2% horse serum and 1 µg/ml insulin after the cells reached about 90% confluence. Differentiating C2C12 cells were supplied with fresh differentiation medium every 24 h and maintained at 37 ^{0}C and 5% CO_2.

Control and *Smyd1* knockdown C2C12 cell lines were generated using GIPZ lentiviral particles encoding short hairpin-RNA against *Smyd1* (Thermo-scientific, source clone ID# V3LMM_480880, V2LMM_61704, V3LMM_480879) and non-silencing control *sh*RNA (catalog # RHS4348) according to the manufacturer's instructions. Successfully transduced cells were selected by puromycin treatment.

***Smyd1 IP and mass spectrometric analysis*.** Antibody specific to Smyd1 was covalently bound to dynabeads (catalog number # 14321 D, Thermo fisher scientific) by overnight incubation, according to the manufacturer's instructions. Quadriceps muscles dissected out of six week old wild type and Smyd1-myf6cre-CKO mice were pulverized in liquid nitrogen and used for immuno-precipitation (IP) of Smyd1 as well as proteins in complex with it through Smyd1 antibody bound to dynabeads. Portion of the eluate from the beads, consisting of immuno-precipitated proteins was used to run a western blot to confirm successful IP of Smyd1. Remaining portion of the eluate was subjected to trypsin digestion leading to fragmentation of isolated proteins. After additional processing using zip-tips, trypsin-digested proteins in solution were analyzed using MALDI-TOF mass spectrometer.

Statistical analyses. For studies with two experimental groups, an independent samples *t*-test was performed. Prior to *t*-test, an F-test was performed to determine if the variances of the two groups were equal. If $P < 0.05$ for the F-test (unequal variances), the test was repeated with log-transformed data. If log-transformed data showed unequal variances, the *t*-test was performed with a correction for unequal variances (Welch test). A *P*-value of < 0.05 was considered significant for all tests.

ACKNOWLEDGEMENTS

The BrdU (G3G4), MyHC (MF-20) and Pax7 and monoclonal antibodies used in this study were obtained from the Developmental Studies Hybridoma Bank, created by the NICHD of the NIH and maintained at The University of Iowa, Department of Biology, Iowa City, IA. This work was supported by the American Heart Association [12BGIA11860006 to M.D.S.]; the University of Houston Division of Research Small Grants Program [1HOU08 to M.D.S.]; and the Texas Heart Institute [M.D.S. and R.J.S.].

Chapter VI

References

REFERENCES

Bentzinger, C. F., Wang, Y. X., and Rudnicki, M. A., 2012. Building Muscle: Molecular Regulation of Myogenesis. Cold Spring Harb Perspect Biol, 4:a008342.

Berkholz, J., Michalick, L., Munz, B., 2014. The E3 SUMO ligase Nse2 regulates sumoylation and nuclear-to-cytoplasmic translocation of skNAC-Smyd1 in myogenesis. J Cell Sci 127, 3794-3804.

Biressi, S., Molinaro, M., Cossu, G., 2007a. Cellular heterogeneity during vertebrate skeletal muscle development. Dev Biol 308, 281-293.

Biressi, S., Tagliafico, E., Lamorte, G., Monteverde, S., Tenedini, E., Roncaglia, E., Ferrari, S., Cusella-De Angelis, M.G., Tajbakhsh, S., Cossu, G., 2007b. Intrinsic phenotypic diversity of embryonic and fetal myoblasts is revealed by genome-wide gene expression analysis on purified cells. Developmental biology 304, 633-651.

Cho, H.S., Hayami, S., Toyokawa, G., Maejima, K., Yamane, Y., Suzuki, T., Dohmae, N., Kogure, M., Kang, D., Neal, D.E., Ponder, B.A., Yamaue, H., Nakamura, Y., Hamamoto, R., 2012. RB1 methylation by SMYD2 enhances cell cycle progression through an increase of RB1 phosphorylation. Neoplasia 14, 476-486.

Coda, D.M., Lingua, M.F., Morena, D., Foglizzo, V., Bersani, F., Ala, U., Ponzetto, C., Taulli, R., 2015. SMYD1 and G6PD modulation are critical events for miR-206-mediated differentiation of rhabdomyosarcoma. Cell Cycle 14, 1389-1402.

Comai, G., Tajbakhsh, S., 2014. Molecular and cellular regulation of skeletal myogenesis. Curr Top Dev Biol.110,1-73.

Du, S.J., Rotllant, J., Tan, X., 2006. Muscle-specific expression of the smyd1 gene is controlled by its 5.3-kb promoter and 5'-flanking sequence in zebrafish embryos. Dev Dyn 235, 3306-3315.

Francetic, T., Li, Q., 2011. Skeletal myogenesis and *Myf5* activation. Transcription 2:3, 109-114.

Gao, J., Li, J., Li, B.J., Yagil, E., Zhang, J., Du, S.J., 2014. Expression and functional characterization of Smyd1a in myofibril organization of skeletal muscles. PLoS One 9, e86808.

Gottlieb, P.D., Pierce, S.A., Sims, R.J., Yamagishi, H., Weihe, E.K., Harriss, J.V., Maika, S.D., Kuziel, W.A., King, H.L., Olson, E.N., Nakagawa, O., Srivastava, D., 2002. Bop encodes a muscle-restricted protein containing MYND and SET domains and is essential for cardiac differentiation and morphogenesis. Nat Genet 31, 25-32.

Haldar, M., Hancock, J.D., Coffin, C.M., Lessnick, S.L., Capecchi, M.R., 2007. A conditional mouse model of synovial sarcoma: insights into a myogenic origin. Cancer Cell 11, 375-388.

Haldar, M., Karan, G., Tvrdik, P., Capecchi, M.R., 2008. Two cell lineages, myf5 and myf5-independent, participate in mouse skeletal myogenesis. Dev Cell 14, 437-445.

Hayashi, S., Tenzen, T., McMahon, A.P., 2003. Maternal inheritance of Cre activity in a Sox2Cre deleter strain. Genesis 37, 51-53.

Huang, J., Perez-Burgos, L., Placek, B.J., Sengupta, R., Richter, M., Dorsey, J.A., Kubicek, S., Opravil, S., Jenuwein, T., Berger, S.L., 2006. Repression of p53 activity by Smyd2-mediated methylation. Nature 444, 629-632.

Hwang, I., Gottlieb, P.D., 1997. The Bop gene adjacent to the mouse CD8b gene encodes distinct zinc-finger proteins expressed in CTLs and in muscle. J Immunol 158, 1165-1174.

Just, S., Meder, B., Berger, I.M., Etard, C., Trano, N., Patzel, E., Hassel, D., Marquart, S., Dahme, T., Vogel, B., Fishman, M.C., Katus, H.A., Strahle, U., Rottbauer, W., 2011. The myosin-interacting protein SMYD1 is essential for sarcomere organization. J Cell Sci 124, 3127-3136.

Kawamura, S., Yoshigai, E., Kuhara, S., Tashiro, K., 2008. smyd1 and smyd2 are expressed in muscle tissue in Xenopus laevis. Cytotechnology 57, 161-168.

Li, D., Niu, Z., Yu, W., Qian, Y., Wang, Q., Li, Q., Yi, Z., Luo, J., Wu, X., Wang, Y., Schwartz, R.J., Liu, M., 2009. SMYD1, the myogenic activator, is a direct target of serum response factor and myogenin. Nucleic Acids Res 37, 7059-7071.

Li, H., Xu, J., Bian, Y.H., Rotllant, P., Shen, T., Chu, W., Zhang, J., Schneider, M., Du, S.J., 2011. Smyd1b_tv1, a key regulator of sarcomere assembly, is localized on the M-line of skeletal muscle fibers. PLoS One 6, e28524.

Li, H., Zhong, Y., Wang, Z., Gao, J., Xu, J., Chu, W., Zhang, J., Fang, S., Du, S.J., 2013. Smyd1b is required for skeletal and cardiac muscle function in zebrafish. Mol Biol Cell 24, 3511-3521.

Luo, X.G., Zhang, C.L., Zhao, W.W., Liu, Z.P., Liu, L., Mu, A., Guo, S., Wang, N., Zhou, H., Zhang, T.C., 2014. Histone methyltransferase SMYD3 promotes MRTF-A-mediated transactivation of MYL9 and migration of MCF-7 breast cancer cells. Cancer Lett 344, 129-137.

Mazur, P.K., Reynoird, N., Khatri, P., Jansen, P.W., Wilkinson, A.W., Liu, S., Barbash, O., Van Aller, G.S., Huddleston, M., Dhanak, D., Tummino, P.J., Kruger, R.G., Garcia, B.A., Butte, A.J., Vermeulen, M., Sage, J., Gozani, O.,

2014. SMYD3 links lysine methylation of MAP3K2 to Ras-driven cancer. Nature 510, 283-287.

Nagy, A., 2003. Manipulating the mouse embryo : a laboratory manual, 3rd ed. Cold Spring Harbor Laboratory Press, Cold Spring Harbor, N.Y.

Phan, D., Rasmussen, T.L., Nakagawa, O., McAnally, J., Gottlieb, P.D., Tucker, P.W., Richardson, J.A., Bassel-Duby, R., Olson, E.N., 2005. BOP, a regulator of right ventricular heart development, is a direct transcriptional target of MEF2C in the developing heart. Development 132, 2669-2678.

Piao, L., Kang, D., Suzuki, T., Masuda, A., Dohmae, N., Nakamura, Y., Hamamoto, R., 2014. The histone methyltransferase SMYD2 methylates PARP1 and promotes poly(ADP-ribosyl)ation activity in cancer cells. Neoplasia 16, 257-264, 264 e252.

Rasmussen, T.L., Ma, Y., Park, C.Y., Harriss, J., Pierce, S.A., Dekker, J.D., Valenzuela, N., Srivastava, D., Schwartz, R.J., Stewart, M.D., Tucker, H.O., 2015. Smyd1 facilitates heart development by antagonizing oxidative and ER stress responses. PLoS One 10, e0121765.

Rossi, G., Messina, G., 2014. Comparative myogenesis in teleosts and mammals. Cell Mol Life Sci 71, 3081-3099.

Rudnicki, M.A., Schnegelsberg, P.N., Stead, R.H., Braun, T., Arnold, H.H., Jaenisch, R., 1993. MyoD or Myf-5 is required for the formation of skeletal muscle. Cell 75, 1351-1359.

Saddic, L.A., West, L.E., Aslanian, A., Yates, J.R., 3rd, Rubin, S.M., Gozani, O., Sage, J., 2010. Methylation of the retinoblastoma tumor suppressor by SMYD2. J Biol Chem 285, 37733-37740.

Sajjad, A., Novoyatleva, T., Vergarajauregui, S., Troidl, C., Schermuly, R.T., Tucker, H.O., Engel, F.B., 2014. Lysine methyltransferase Smyd2 suppresses p53-dependent cardiomyocyte apoptosis. Biochim Biophys Acta 1843, 2556-2562.

Sims, R.J., 3rd, Weihe, E.K., Zhu, L., O'Malley, S., Harriss, J.V., Gottlieb, P.D., 2002. m-Bop, a repressor protein essential for cardiogenesis, interacts with skNAC, a heart- and muscle-specific transcription factor. J Biol Chem 277, 26524-26529.

Spellmon, N., Holcomb, J., Trescott, L., Sirinupong, N., Yang, Z., 2015. Structure and function of SET and MYND domain-containing proteins. Int J Mol Sci 16, 1406-1428.

Wagner, J., Schmidt, C., Nikowits, W Jr., Christ, B., 2000. Compartmentalization of the somite and myogenesis in chick embryos are influenced by wnt expression. Dev Biol 228(1), 86-94.

Tan, X., Rotllant, J., Li, H., De Deyne, P., Du, S.J., 2006. SmyD1, a histone methyltransferase, is required for myofibril organization and muscle contraction in zebrafish embryos. Proc Natl Acad Sci U S A 103, 2713-2718.

Xu, G., Liu, G., Xiong, S., Liu, H., Chen, X., Zheng, B., 2015. The histone methyltransferase Smyd2 is a negative regulator of macrophage activation by suppressing interleukin 6 (IL-6) and tumor necrosis factor alpha (TNF-alpha) production. J Biol Chem 290, 5414-5423.

Yang, J., Everett, A.D., 2009. Hepatoma-derived growth factor represses SET and MYND domain containing 1 gene expression through interaction with C-terminal binding protein. J Mol Biol 386, 938-950.

Zouraq, F. A., Stölting, M., Eberli, D., 2013. Skeletal Muscle Regeneration for Clinical Application, Regenerative Medicine and Tissue Engineering. ISBN: 978-953-51-1108-5.

Stewart, M.D., Lopez, S., Nagandla, H., Soibam, B., Benham, A., Nguyen, J., Valenzuela, N., Wu, H.J., Burns, A.R., Rasmussen, T.L., Tucker, H.O., Schwartz, R.J., 2015. Skeletal muscle-specific loss of the SMYD1 methyltransferase causes centronuclear myopathy. *Unpublished manuscript*.